NASA TECHNICAL NOTE

NASA TN D-1996

NASA TN D-1996

ESTIMATION OF TOLERANCE LIMITS FOR METEOROID HAZARD TO SPACE VEHICLES 100-500 KILOMETERS ABOVE THE SURFACE OF THE EARTH

by Charles C. Dalton

George C. Marshall Space Flight Center
Huntsville, Alabama

NATIONAL AERONAUTICS AND SPACE ADMINISTRATION • WASHINGTON, D. C. • FEBRUARY 1964

ESTIMATION OF TOLERANCE LIMITS FOR METEOROID HAZARD TO SPACE VEHICLES 100-500 KILOMETERS ABOVE THE SURFACE OF THE EARTH

By Charles C. Dalton

George C. Marshall Space Flight Center
Huntsville, Alabama

NATIONAL AERONAUTICS AND SPACE ADMINISTRATION

For sale by the Office of Technical Services, Department of Commerce,
Washington, D.C. 20230 -- Price $1.50

TABLE OF CONTENTS

LIST OF ILLUSTRATIONS (Cont'd)

LIST OF TABLES

LIST OF SYMBOLS

Symbol	Definition
A	Square meters effectively exposed vehicle area; e.g., half of the area of a spherical vehicle.
t	Duration of exposure in seconds.
p	Thickness of a just-puncturable metallic shell under given impact conditions in centimeters.
ρ_t	Density of the wall of the space vehicle (target) in grams per cubic centimeter.
H_t	Brinell Hardness of the target material.
m	Meteoroid mass in grams.
ϕ	Mean puncture flux per square meter per second.
R	Probability that an exposed area A will not be punctured during time t.
C	One-sided confidence level.
f(t)	Probability density functions for puncture at time t.
m(t)	Specific mortality function for puncture at time t.
x_2	Meteoroid zenity angle at impact, radians, random variable.
r_a	Geocentric radial distance to outer edge of Earth's atmosphere implicit in meteor velocity data.
r	Geocentric radial distance to an orbiting spacecraft.
v_a	Velocity of a meteoroid at geocentric radial distance r_a relative to the Earth's atmosphere in km/sec
km	Kilometers
sec	Second

Symbol	Definition
v_r	Velocity of a meteoroid at geocentric radial distance $r \geq r_a$ relative to the Earth's atmosphere.
v_∞	Meteoroid hyperbolic velocity excess with respect to the Earth.
m_e	Mass of the Earth.
γ	Universal gravitational constant.
D_{x_1}	Displacement of the center of the Earth from an asymptote of the hyperbolic trajectory of a meteoroid.
v_e	Escape velocity at geocentric radial distance r.
$F_>$	Flux of meteoroids of mass equal to or greater than m; mean number of hits per square meter of effectively exposed surface area.
β_3	Flux intercept; value of $\log_{10} F_>$ for m = 1 (gram).
β_2	Slope of line relating common logarithms of $F_>$ and m.
Z_{AR}	Angle between the meteor apparent radiant and the station zenith.
Z	Angle between the meteor at maximum brilliance and the station zenith.
M_V	Meteor absolute visual magnitude.
M	Meteor apparent visual magnitude.
M_{pm}	Meteor maximum photographic absolute magnitude.
h	Meteor height in kilometers at maximum brilliance.
f_i	Weighting factor for the i^{th} meteor in a sample.
gm	Gram.
y_2	Geocentric velocity intercept; value of $\log_{10} v_a$ for m = 1 gm; random variable.
β_4	Slope of line relating common logarithms of v_a and m.

LIST OF SYMBOLS (Concl'd)

Symbol	Definition
v_s	Vehicle orbital velocity in km/sec.
v_c	Closing velocity between a meteoroid and a vehicle in a near-Earth orbit.
y_3	Closing velocity exponent; random variable.
ρ_p	Meteoroid or projectile density in grams per cubic centimeter.
β_1	Meteoroid median density.
y_1	Meteoroid density exponent; random variable.
cm	Centimeter.
y_4	Velocity exponent in crater depth formula; random variable
β_5	Mass exponent in crater depth formula
p_o	Crater depth in a thick target; centimeters.
x_2	Angle of impact relative to the normal to the surface, $0 \leq x_2 \leq \frac{1}{2} \pi$ radians; random variable.
d	Meteoroid diameter in centimeters.
y_5	Exponent of the coefficient in the formula for p_o/d; random variable.
p	Thickness of a just-puncturable shell under given impact conditions; centimeters.
y_6	The common logarithm of the ratio of puncturable thickness and crater depth; random variable.
y_7	The common logarithm of the coefficient of puncturable thickness; random variable.
y_9	The common logarithm of the coefficient of puncture flux; random variable.

ACKNOWLEDGMENT

The analysis described in this report is one phase of an Aero-Astrodynamics Laboratory in-house effort. The necessary supporting services were provided by the Aero-Astrophysics Office. Mr. Frank D'Arcangelo prepared all of the illustrations and compilations and obtained and checked the necessary computations, which were programmed by Miss Sylvia Bowers for a GE 225 digital computer. Suggestions by Dr. E. D. Geissler (Director, Aero-Astrodynamics Laboratory), Dr. W. H. Heybey and Mr. W. D. Murphree (Scientific Assistants), and Mr. W. W. Vaughan (Chief, Aero-Astrophysics Office) have been very helpful.

NATIONAL AERONAUTICS AND SPACE ADMINISTRATION

TECHNICAL NOTE D-1996

ESTIMATION OF TOLERANCE LIMITS FOR METEOROID HAZARD TO SPACE VEHICLES 100-500 KILOMETERS ABOVE THE SURFACE OF THE EARTH

By

Charles C. Dalton

SUMMARY

Most of the uncertainty in the meteoroid puncture hazard for vehicles near the Earth is attributable to the uncertainty in meteoroid density (specific gravity). There is an even chance that density is between 0.094 and 2.1.

All meteoroids which approach the Earth from interplanetary space (the only case considered in this paper) experience a velocity increment equal to the escape velocity, which is 11 km/sec near the Earth. Half of the meteoroids have atmospheric impact velocities between 19 and 47 km/sec. The paths of the relatively slower meteoroids are deflected more by the gravitational field of the earth so that the collision cross section for the Earth is relatively larger. For instance, those meteoroids which have near-Earth velocities only 5 percent greater than escape velocity have more than an order of magnitude greater flux near the Earth than in interplanetary space. But the statistical distribution of the zenith angle for all meteoroids which collide with the atmosphere is invariant with respect to velocity. Therefore the zenith angles have decrements which are appreciable for relatively slow meteors.

The number of photographic meteors increases by a factor of approximately 26 for an order of magnitude decrease in meteoroid relative mass. But the absolute value of mass is not accurately known. There is only an even chance that the average flux of meteoroids of mass greater than an indicated mass can be specified between limits which are separated by 3.8 orders of magnitude.

When the velocity of a meteoroid is not specified, the thickness of a just-puncturable wall is directly proportional to the cube root of the meteoroid mass and inversely proportional to the cube root of the product of the density and Brinell hardness

of the wall material. There is an even chance that the proportionality constant is between 7.8 and 26 when meteoroid mass and wall thickness are in grams and centimeters, respectively.

For a vehicle which is nearly spherical or which has random attitude, the average number of punctures per square meter of effectively exposed area per second in a near-Earth orbit is inversely proportional to the 1.42 power of the product of the density, the Brinell hardness, and the cube of the thickness of the wall. There is an even chance that, with wall thickness expressed in centimeters, the proportionality constant is between 2.2×10^{-13} and 1.6×10^{-7}. Shielding by the Earth may reduce the effectively exposed area to about half the total area.

For achieving a specified design reliability for a specified mission, there is an even chance that the wall thickness of a space vehicle can be specified between lower and upper limits that are separated by 1.4 orders of magnitude. The confidence in achieving the required no-puncture probability can be increased from 50 percent to 73 percent by making the single wall 4.4 times thicker. It may be that the same advantage could be gained by using two thinner walls of the same total thickness separated by one inch of glass wool filler.

A least-squares analysis of data for a random sample of 286 photographic sporadic meteors with masses spanning three orders of magnitude gives a correlation of -0.82 between the logarithms of mass and velocity. The significant negative correlation did not change when special weighting factors were used.

SECTION I. INTRODUCTION

A. SCOPE

The information which is included in the selected references which are cited at the end of this report was reviewed as a perspective basis for decisions about: (1) what parameters are appropriate for representing meteoroid hazard, and (2) what are the most convenient functional relations and statistical representations which would not appear to bias the end results.

It is assumed: (1) that the vehicle is either spherical or that it does not have attitude control, (2) that all segments of the wall of the vehicle are equally important and that they are of the same material and thickness, and (3) that the day and hour of the exposure have not been related to specific forecasts of meteoroid flux (shower events, seasonal, and diurnal variations).

Single-shell-of-metal is the basis of the analysis. Of course, there is considerable interest in composite bumpers and, e.g., in multiple-sheet structures [Ref. 2]; but it is hoped that the effectiveness of other materials and structures can be considered in terms of the effectiveness of some thickness of single-shell-of-metal.

B. METHOD

The value that a physical parameter (e.g., length, velocity, etc.) will have under specified circumstances will be uncertain when: (1) the parameter (or the physical process of which the parameter is indicative) may be capricious (e.g., the parameter may be a random statistical variable), (2) the available information may not be either sufficiently firm or direct, or (3) the latter is compounded with the former - as in the present problem - the resulting uncertainty being treated as if it were caused by randomness.

C. MATHEMATICAL CONSIDERATIONS

Several of the random variables are introduced as exponents rather than as coefficients because they involve decisions concerning the relation between the logarithms of parameters.

The confidence C in the antilogarithm of an approximately normally distributed chance variable y is the same as the confidence in the variable; i.e.,

$$(C,\ 10^{y}) = (0.25,\ 10^{\bar{y}-0.6745\sigma_y}),\ (0.50,\ 10^{\bar{y}}),$$

$$(0.75,\ 10^{\bar{y}+0.6745\sigma_y}). \qquad (1)$$

SECTION II. INTERPRETATION OF THE INFORMATION FROM SELECTED REFERENCES

A. METEOROID DENSITY

Meteoroids differ not only in mass, but also those which have approximately the same mass may differ widely in composition and structure. They are, in the order of increasing abundance and decreasing puncturability, classified broadly as: (1) metallic, with density somewhat more or less than that of iron, say $\rho_p = 7.8$, (2) stony, say with density somewhat more or less than $\rho_p = 3.5$, and (3) fluffy, with density somewhat more or less than the value

$$\beta_1 = 0.443 \qquad (2)$$

recently suggested by Whipple [3]. In this analysis the meteoroid density is represented by a random variable (which is also considered to be the source of the uncertainty in meteoroid flux in Section II. B. 4) with normally distributed common logarithm, the mean value of which agrees with Eq. 2 and the variance of which is unity, i.e.,

$$\rho_p = 10^{y_1}, \tag{3}$$

$$\overline{y}_1 = \log_{10} \beta_1 = -0.354, \tag{4}$$

$$\sigma_{y_1} = 1.00 \tag{5}$$

B. METEOROID FLUX

1. Temporal Dependence of Flux. The probability density function f(t) for the meteoroid puncture of a space vehicle is

$$f(t) = m(t)\, e^{-\int_0^t m(t)\, dt} \tag{6}$$

where m(t) is a function of time which in life statistics is called "specific mortality" and in engineering statistics is sometimes called "failure-rate-of-survivors" or "hazard function." Then the product m(t) dt is the conditional probability that if the event has not already occurred by time t then it will occur in the interval between t and t + dt. The probability R that the event will not have occurred by time t is

$$R = 1 - \int_0^t f(t)\, dt = e^{-\int_0^t m(t)\, dt} = e^{-\int_0^t \phi A\, dt} \tag{7}$$

where A is the effectively exposed area of the vehicle in square meters, and the flux ϕ is the number of puncturable meteoroids per square meter per second.

The specific mortality function corresponding to the Poisson distribution function is the constant reciprocal of the mean-time-to-occurrence for the repeated event, i.e., m is the average rate of occurrence of the event, or in meteoroid technology, flux ϕ times exposed area A, and Eq. 7 becomes

$$R = e^{-\phi A t}. \tag{8}$$

For either sporadic or shower meteoroids, impact probability is sufficiently approximated by either a Poisson or a piece-wise-Poisson description with respect to

time, depending on whether the available information is specific or general, and on whether one is concerned with specific or average circumstances. But the combined effect for two such hazards also has a Poisson description:

$$R = e^{-A}\left[(\phi_{11} + \phi_{12})\,t_1 + (\phi_{21} + \phi_{22})\,t_2 + \cdots + (\phi_{n1} + \phi_{n2})\,t_n\right]. \qquad (9)$$

Eqs. 8 and 9 give the same result for the same exposure At whenever ϕ in Eq. 8 is the time average of the $\phi_1, \cdots \phi_n$ in Eq. 9. It does not make any difference whether or not the ϕ in Eq. 8 and the $\phi_1, \cdots, \phi_n$ in Eq. 9 are further resolved into: (1) components due to sporadic meteoroids, and (2) components due to shower meteoroids -- unless it should be found that the two populations should be separately described with respect to mass, density, velocity, etc.

2. Directional Dependence of Flux. Since this analysis is only for meteoroid hazard near the Earth, and since most of the information on which the analysis is based is from meteoroids incident onto a space vehicle or into the atmosphere, the distributions of the orbital elements of the meteoroids (e.g., perihelion, eccentricity, inclination from the plane of the ecliptic, etc.) do not need to be established. Rather, one is concerned about the zenith angle x_1, i.e., the angle between the geocentric position vector of the meteoroid and the negative of its geocentric closing velocity vector.

The necessary functional relations for hyperbolic trajectories are given in introductory treatments of celestial mechanics. The hyperbolic velocity excess v_∞ is

$$v_\infty = (v_a^2 - 2\gamma m_e / r_a)^{\frac{1}{2}}, \qquad (10)$$

where m_e is the mass of the Earth, γ is the universal constant of gravitation, and r_a is the radial distance from the center of the Earth to the zone implicit in meteoroid velocity data. The velocity v_r at radial distance r is, by Eq. 10,

$$v_r = \left[v_a^2 - 2\gamma m_e \left(\frac{1}{r_a} - \frac{1}{r}\right)\right]^{\frac{1}{2}}. \qquad (11)$$

Since a spacecraft orbits at geocentric radial distance r, it is convenient to consider that a geocentric sphere of radius r makes a tunnel of radius $D_{\frac{1}{2}\pi}$ through a swarm of meteoroids. This is true when (1) the trajectory of any meteoroid originally approaching along the surface of the tunnel with the closing velocity v_∞ is tangent to the sphere r, and when (2) the trajectory of any meteoroid originally approaching with the same velocity but within the tunnel and displaced only $D_{x_1} < D_{\frac{1}{2}\pi}$ from the tunnel axis cuts the

sphere r at angle $x_1 < \frac{1}{2}\pi$ with respect to the local position vector (i.e., x_1 is the zenith angle). Because of the conservation of angular momentum, the cross product of the meteoroid velocity vector and geocentric radius vector is invariant with respect to the position of any particular meteoroid along its trajectory, i.e.,

$$v_\infty D_{x_1} = v_r \, r \sin x_1 \ . \tag{12}$$

The potential energy of a meteoroid at radial distance r is invariant with respect to zenith angle x_1, and, because of the conservation of total energy, the kinetic energy is also invariant. The velocity v_r is also invariant with respect to mass for given v_∞. Then v_r and, therefore, $v_r r$ are invariant with respect to x_1. Substituting $\pi/2$ for x_1 in Eq. 12 gives

$$\left.\begin{aligned} v_r r &= v_\infty D_{\pi/2} \\ \sin x_1 &= D_{x_1} / D_{\pi/2} \end{aligned}\right\} \tag{13}$$

Since the relative area of a narrow concentric ring in the cross section of the tunnel is equal to the product of its relative circumference and its differential relative width, and because of diurnal averaging, one must admit equal probability for positive and negative values of x_1. It follows from Eq. 13 that the probability distribution function for x_1, $-\frac{1}{2}\pi \leq x_1 \leq \frac{1}{2}\pi$, is

$$f(x_1) = \left| (2\pi \sin x_1) \frac{d}{dx_1} (\sin x_1) \, / 2\pi \right| = \frac{1}{2} \left| \sin 2x_1 \right| . \tag{14}$$

Therefore, the mean and standard deviation of x_1 are:

$$\overline{x_1} = 0, \tag{15}$$

and

$$\sigma_{x_1} = [(\pi^2 - 4) / 8]^{\frac{1}{2}} = 0.856 \text{ radians.} \tag{16}$$

Although the above tunnel concept was convenient in the derivation of Eqs. 13 through 16, the results should be valid (on a diurnal average basis) also when meteoroids approach the Earth from any direction. By Eq. 13 one sees that half of the meteors should approach the atmosphere with angles deviating less than 45 degrees from the zenith.

Hawkins and Southworth [1] tabulated values of cos Z_{AR}, velocity v_a, and maximum photographic absolute magnitude M_{pm}, where Z_{AR} is the apparent radiant zenith angle for a random sample of 286 sporadic meteors selected from the Baker Super-Schmidt photographs taken from stations in New Mexico from February 1952 to July 1954.

Meteor radiant zenith angles Z_{AR} calculated from those data have the following mean and standard deviation when the data are uniformly weighted:

$$\overline{Z}_{AR} = 0.64 \text{ radians} \tag{17}$$

$$\sigma_{Z_{AR}} = 0.30 \text{ radians} \tag{18}$$

But, by Eq. 14, the mean and standard deviation of arithmetic values of meteoroid zenith angles x_1 should be $\pi/4 = 0.79$ and 0.34, respectively.

The sample cumulative probability contour for uniformly weighted meteor radiant zenith angle Z_{AR} and the theoretical cumulative probability contour for the arithmetic value of the meteoroid velocity vector zenith angle $|x_1|$ are both shown in Figure 1 for further comparison. Apparently the sample of meteor radiants is considerably biased with respect to zenith angle Z_{AR} in that large angles are not sufficiently represented (the sample spans the interval $0 \leq Z_{AR} \leq 80°$). Although this bias could be caused by the limitations of the field of view of the cameras, it must be attributed, at least in part, to atmospheric attenuation.

By the method of non-uniform weighting developed in Appendix A, the same calculated values of Z_{AR} have the following mean and standard deviation:

$$\overline{Z}_{AR} = 0.59 \tag{19}$$

$$\sigma_{Z_{AR}} = 0.29; \tag{20}$$

and the sample cumulative probability contour is shown in Figure 2.

Apparently the distribution of meteor apparent zenith angles is not appreciably influenced by the weighting scheme, which is used for a different purpose, thus affording some reassurance that the weighting scheme may not introduce devious complications.

3. Spatial Dependence of Flux. By Eqs. 10, 11, and 13, the factor by which the flux of meteoroids is increased at geocentric radial distance r by the gravitational field is

$$\left(\frac{D_{\pi/2}}{r}\right)^2 = \left(\frac{v_r}{v_\infty}\right)^2 = 1 + \left(\frac{v_e}{v_\infty}\right)^2 = \left[1 - \left(\frac{v_e}{v_r}\right)^2\right]^{-1} \tag{21}$$

where v_e is the escape velocity at the distance of interest r. For instance, the flux of those meteoroids which enter the atmosphere with geocentric velocity only 5 percent in

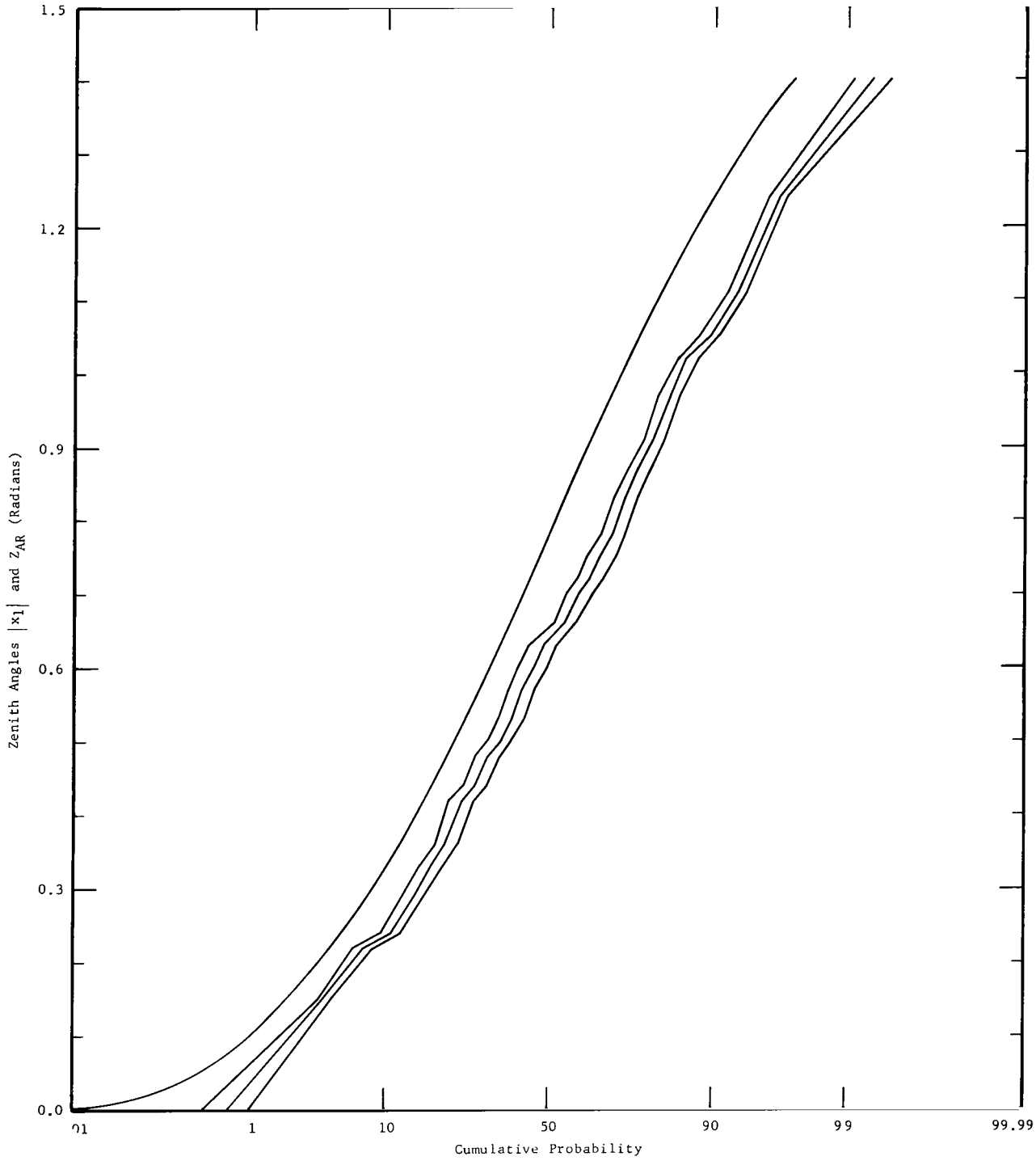

FIGURE 1. CUMULATIVE PROBABILITY FOR ZENITH ANGLE $|x_1|$ OF DIURNAL METEOROIDS AND CUMULATIVE PROBABILITY QUARTILES FOR ANGLE Z_{AR} BETWEEN THE ZENITH AND THE APPARENT RADIANTS OF SPORADIC NOCTURNAL METEORS (REF. 1). UNIFORM WEIGHTING.

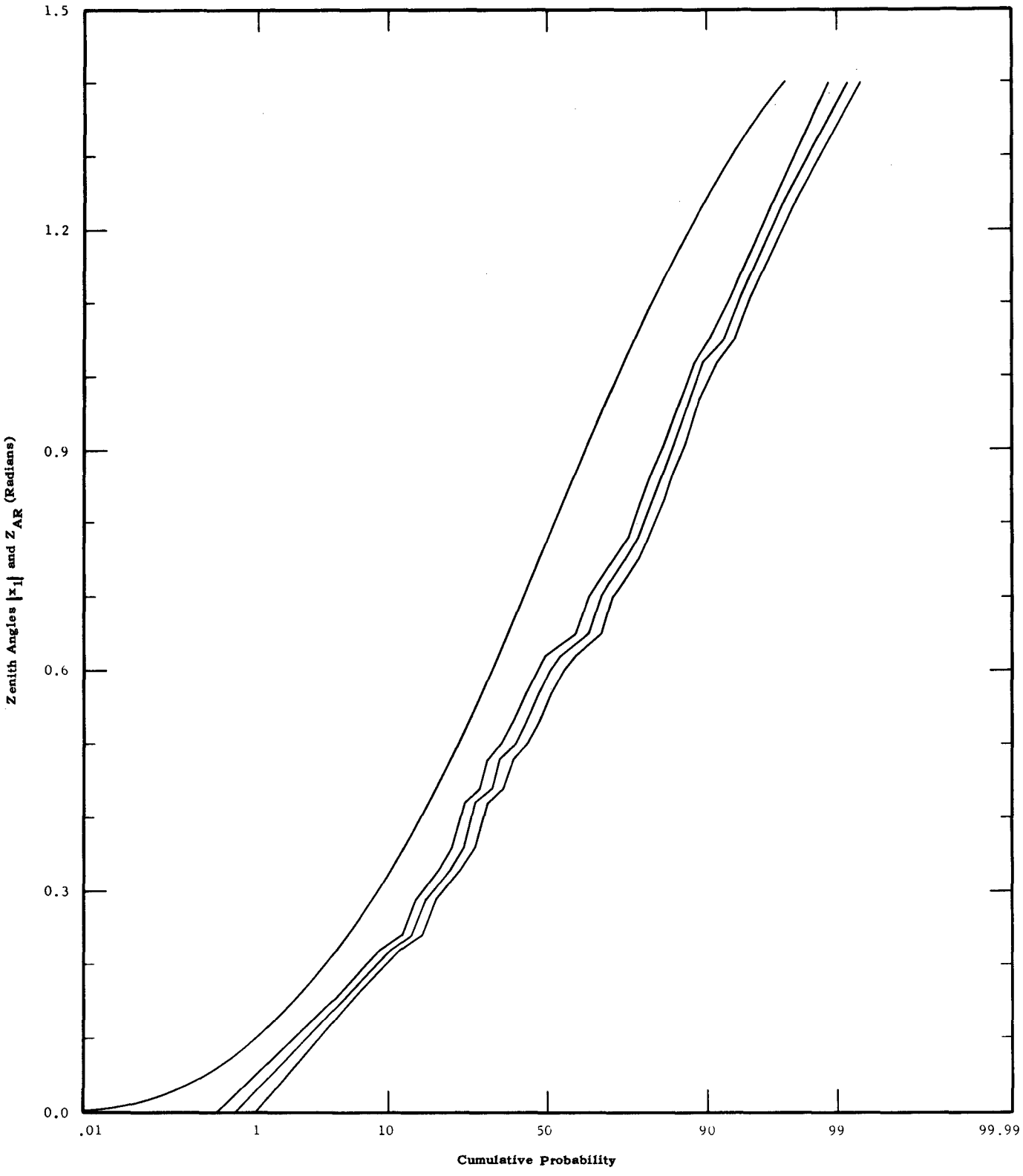

FIGURE 2. CUMULATIVE PROBABILITY FOR ZENITH ANGLE $|x_1|$ OF DIURNAL METEOROIDS AND CUMULATIVE PROBABILITY QUARTILES FOR ANGLE Z_{AR} BETWEEN THE ZENITH AND THE APPARENT RADIANTS OF SPORADIC NOCTURNAL METEORS (REF. 1) NON-UNIFORM WEIGHTING.

excess of the escape velocity is increased by more than one order of magnitude. This focusing efficiency is a monotonically decreasing function of geocentric radial distance; but it may be more than enough to compensate for the monotonically decreasing shielding of a vehicle by the Earth.

4. Mass Dependence of Flux. An equation of the form

$$F_{>} = \alpha\, m^{\beta_2} \tag{22}$$

is used by many investigators. $F_{>}$ is the flux of particles having mass m or greater, and α and β_2 are constants.

The selection of a solution pair of values (α , β_2) is not decided in the $F_{>}$,m domain by most authors. It is decided in the $\log_{10} F_{>}$, $\log_{10}$ m domain; i.e., from a family of equi-probable contours of possible solution points which are the consequences of the following underlying functional representation

$$\log_{10} F_{>} = \beta_2 \left[\log_{10} m + 2\log_{10}(\beta_1/\rho_p)\right] + \beta_3 \quad . \tag{23}$$

Functional relations between the flux $F_{>}$ of meteoroids with masses equal to or greater than m to be encountered by a spacecraft, or relations between $\log_{10} F_{>}$ and $\log_{10} m$, have been inferred primarily from data obtained by careful quantitative measurements of physical parameters involved in the following four phenomena: (1) the interaction of meteoroids with the atmosphere of the Earth as studied by visual, photographic, and radar methods and discussed by Whipple [4], (2) the accumulation of meteoroid debris on the Earth as studied by chemical, physical, and statistical analyses of the sediments, and discussed by Laevastu and Mellis [5], (3) the disturbance by micrometeoroids hitting instrumented artificial satellites as studied by microphones, and discussed by Dubin [6 and 7], and (4) interaction between micrometeoroids and electromagnetic radiation, as implied by physical optical peculiarities of solar corona and zodiacal light, and discussed by Beard [8]. The combined interpretation of these four separate categories of information is further facilitated (or confused, depending on one's point of view) by theoretical considerations of the paths of meteoroids of given mass and cross sectional area moving under the combined influences of solar radiation and solar and planetary combined gravitational fields -- as discussed by Siedentopf [9], Best [10] and Beard [8].

The various published interpretations of the preceding information differ considerably, suggesting that the results must yet be uncertain to a considerable extent. When various interpretations are considered as points in a graph, $\log_{10} F_{>}$ versus $\log_{10} m$, then results are missing for 10^{-7} gm < m < 10^{-4} gm. Except for the degradation of optical surfaces, thin films, paints, etc., this is the entire region of interest -- mass m possibly large enough for penetration of a space vehicle (or vital component) and flux

$F_>$ possibly too high to be ignored. None of the various phenomena or underlying principles of interpretation give points on both sides of the interval of interest.

A value for β_3 can be established from data relating meteor flux and meteor visual magnitude after a value has been assumed for m_θ (the mass of a meteoroid which produces a zero visual magnitude meteor). The values of m_0 and v_0 which are assumed (for a meteoroid which enters normally into the atmosphere with 35 km/sec velocity and 0.073 density) for this analysis are

$$m_0 = 10^{\frac{1}{2}(\log_{10} 30 + \log_{10} 1)} = 5.48 \text{ grams}, \tag{24}$$

$$v_0 = 35 \text{ km/sec} \quad . \tag{25}$$

In the random sample of photographic meteor data described in Section II. A. 2, Hawkins and Southworth [1] did not tabulate estimates of the initial masses of the meteoroids corresponding to the meteors. But corresponding values of mass can be inferred. They [1] indicate that absolute photographic magnitude M_{pm} can be converted to absolute visual magnitude M_v by adding an index varying between 1.8 for bright meteors and 1.0 for faint ones. The uniform application of this relation over the sample range $-2.5 \leq M_{pm} \leq 3.3$ can be expressed by

$$M_v = 1.45 + 0.86\, M_{pm} \tag{26}$$

Therefore, with the basic theory of the meteoric process which they [1] presented, and with the values of m_0 and v_0 from Eqs. 24 and 25, one can infer that

$$\log_{10} m = 4.79 - 0.34\, M_{pm} - \log_{10} (v_a^{\,3} \cos Z_{AR}) \quad . \tag{27}$$

The mass dependence of the common logarithm of the sample cumulative probability for the (Eq. 27) uniformly weighted values of $-\log_{10} m$ is illustrated graphically in Figure 3. Except for noise (randomness) and any bias in the sample with respect to meteoroid mass and sample size, the slope of the contour in Figure 3 should have a constant value equal to β_2 in Eq. 23. This follows from Eq. 23, by neglecting the term because of density variations, because the number n_t meteoroids with mass not less than that of the smallest of the sample m_L is proportional to the corresponding cumulative flux $F_{>L}$ times the product of the observed area and duration. The number n_f of meteoroids with mass $m \geq m_1 > m_L$ is the same fraction of n_t as $F_{>1}$ is of $F_{>L}$; i.e., as the ratio of the masses to the power β_2. The corresponding results by the method of non-uniform weighting which is developed in Appendix A are illustrated in Figure 4. The slopes of the median contours in Figures 3 and 4 are -1.19 and -1.42, respectively, when only the fifteen points corresponding to the greatest mass on the logarithmic cumulative probability curve are considered for each case by the

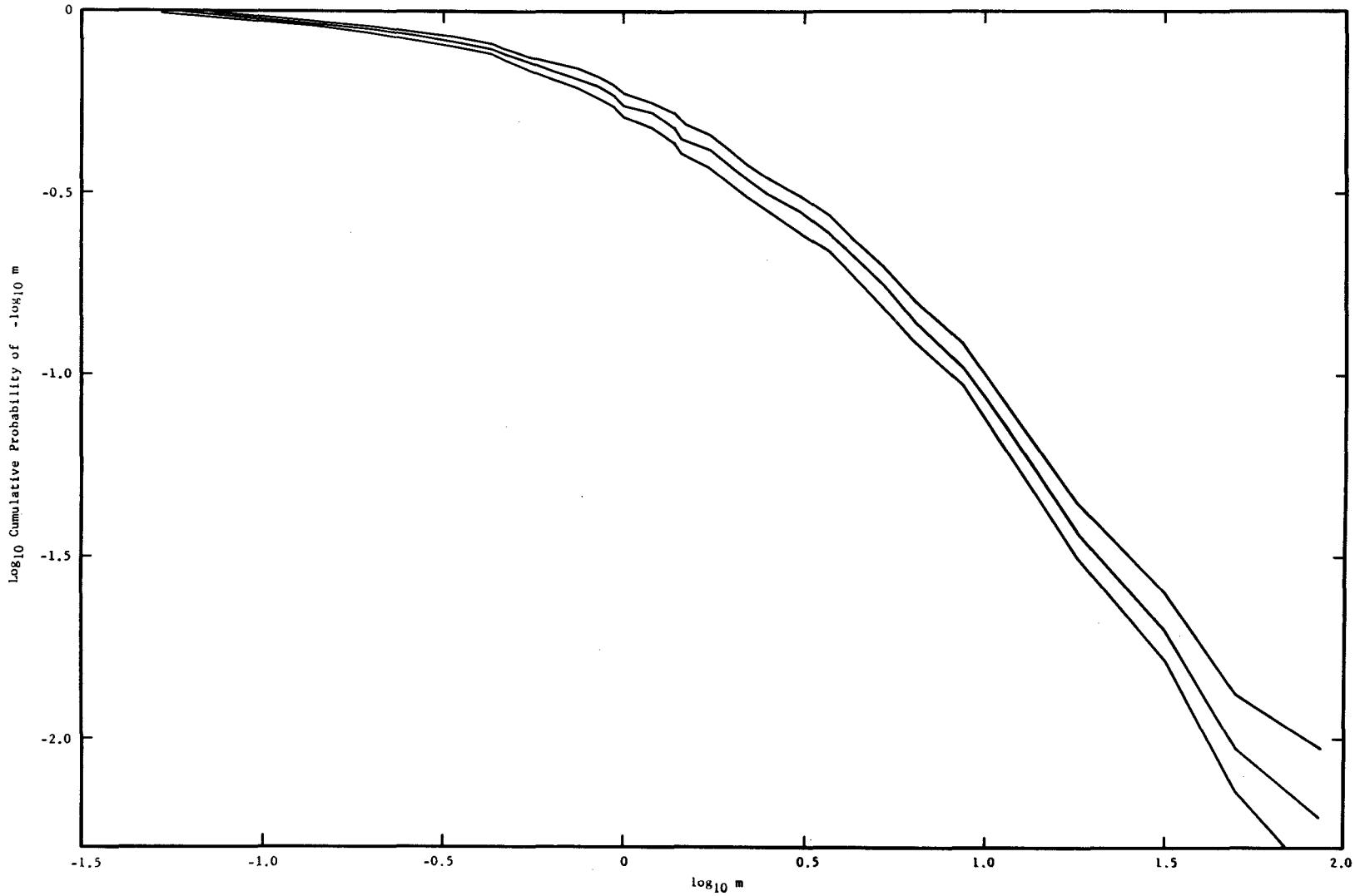

FIGURE 3. QUARTILES OF THE LOGARITHM OF CUMULATIVE PROBABILITY FOR THE LOGARITHM OF RECIPROCAL MASS OF SPORADIC NOCTURNAL METEORS (REF. 1) UNIFORM WEIGHTING.

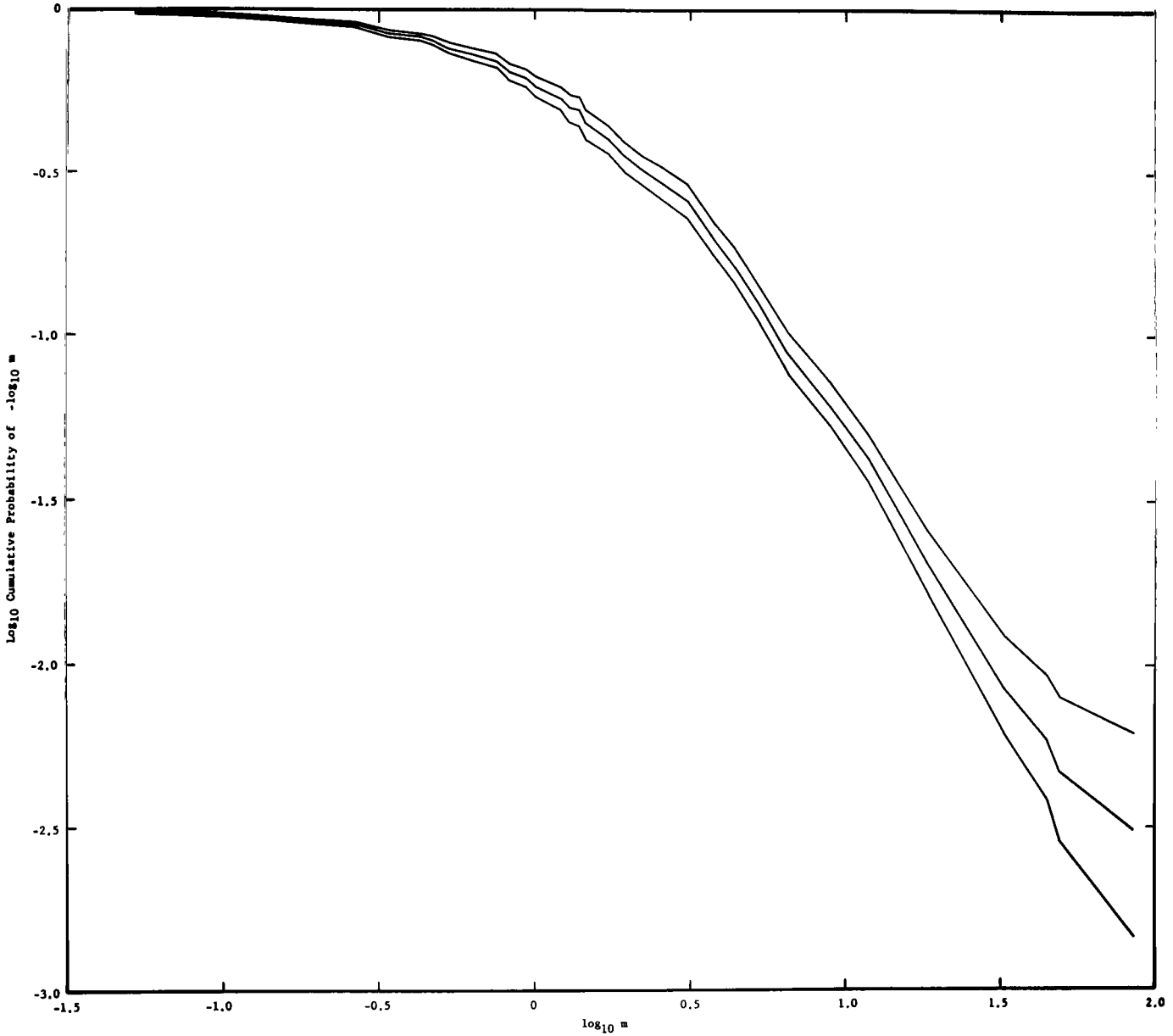

FIGURE 4. QUARTILES OF THE LOGARITHM OF CUMULATIVE PROBABILITY FOR THE LOGARITHM OF RECIPROCAL MASS OF SPORADIC NOCTURNAL METEORS (REF. 1) NON-UNIFORM WEIGHTING.

method of least squares. It would appear that the first fifteen points from the ordered sample may provide a nearly optimum compromise between (1) having enough points for smoothing out any gross irregularities and (2) avoiding that part of the curve which is necessarily curved because the sample size is not relatively large. The appropriate value for β_2 to be used in Eq. 23 is the one from Figure 4,

$$\beta_2 = -1.42, \tag{28}$$

in which the bias with respect to mass has been minimized by using weighting factors. Because the value of β_2 in Eq. 28 differs quite significantly from the alternative value (-1.19), the scatter-diagrams in Figures 5 through 7 are included so that the role of the weighting factors can be more clearly seen.

Based on the assumption that a meteoroid of 0.073 gm/cm^3 density and 35 km/sec velocity normally incident onto the top of the atmosphere will produce a meteor of zero absolute visual magnitude when the mass (Eq. 24) is 5.48 gm, it follows by Eqs. 26 and 27 that Hawkins and Southworth's [1] photographic meteor data can be inferred to relate absolute magnitude to mass according to the scatter diagrams in Figure 8. This is true because absolute magnitude is related to velocity according to the scatter diagram in Figure 9. But the Eq. 28 value for β_2 is invariant both with respect to the Eq. 24 value for m_0 and with respect to any errors in either of Eqs. 26 and 27 which might be caused by the omission of constant terms.

Whipple [3] suggests the following values for the constants in Eq. 23:

$$(\beta_1, \beta_2, \beta_3) = (0.443, -1.34, -14.48)$$

and also indicates that, by adopting the same value for β_2, the corresponding values for the older Watson Law [11] become

$$(\beta_1, \beta_2, \beta_3) = (0.443, -1.00, -13.80).$$

Eq. 23 is invariant with respect to the two sets of values of the constants when m = 10^{-2} grams. This value is within the range usually considered to represent the visual, photographic, and radar meteor phenomena on which both authors [3, 11] based their estimates. By using the values of β_1 and β_2 from Eqs. 32 and 28, the value of β_3 which is considered for this analysis is the value with which the cumulative flux $F_>$ in Eq. 23 is the same as both Whipple [3] and Watson [11] have indicated for m = 10^{-2} grams; i.e.,

$$\beta_3 = -14.64 \ . \tag{29}$$

By Eqs. 23 and 3 it follows that $\log_{10} F_>$ is a linear function of the normally distributed random variable y_1, and is therefore also normally distributed; and, by

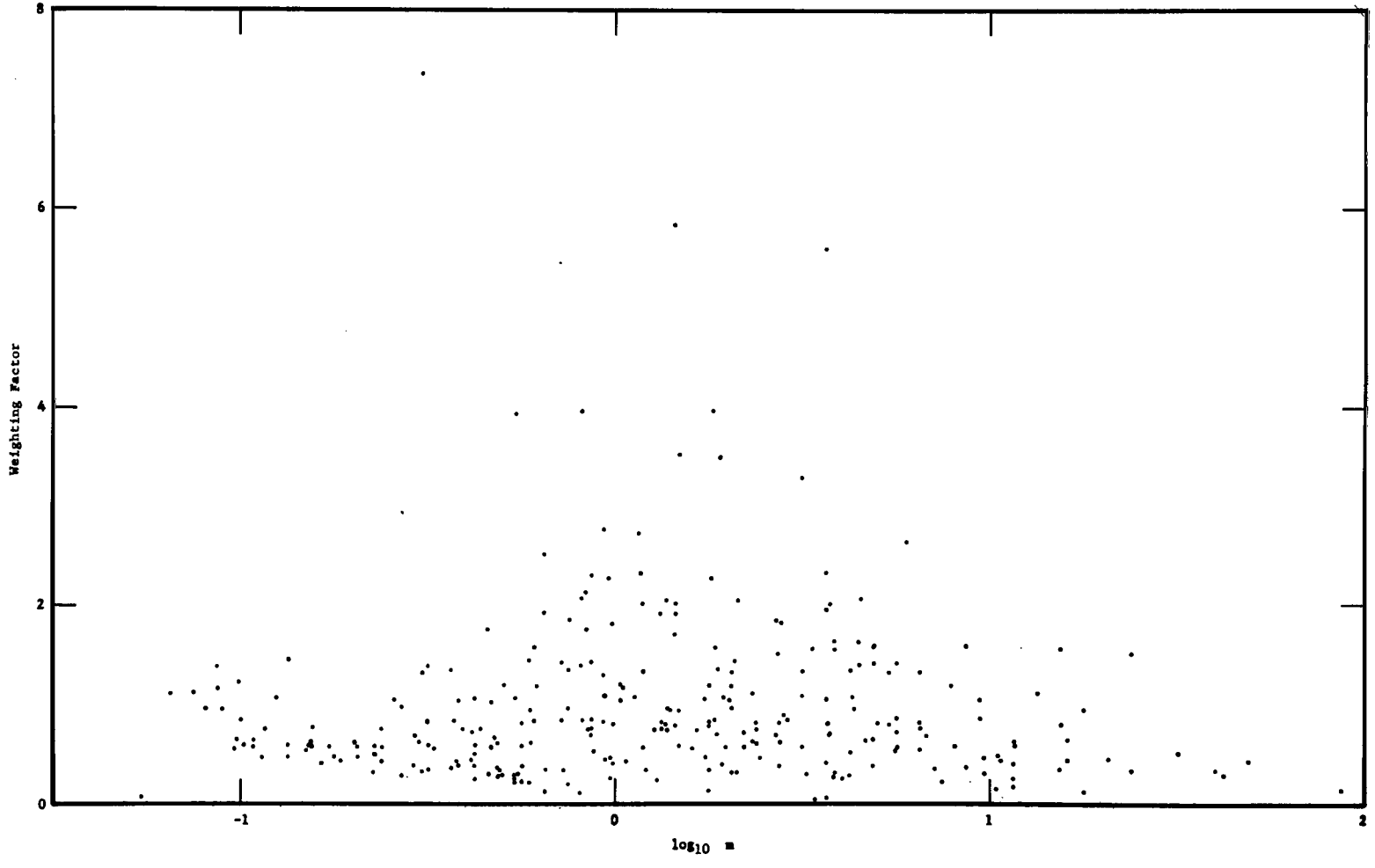

FIGURE 5. MASS-DEPENDENCE OF WEIGHTING FACTORS FOR SPORADIC NOCTURNAL METEORS (REF. 1).

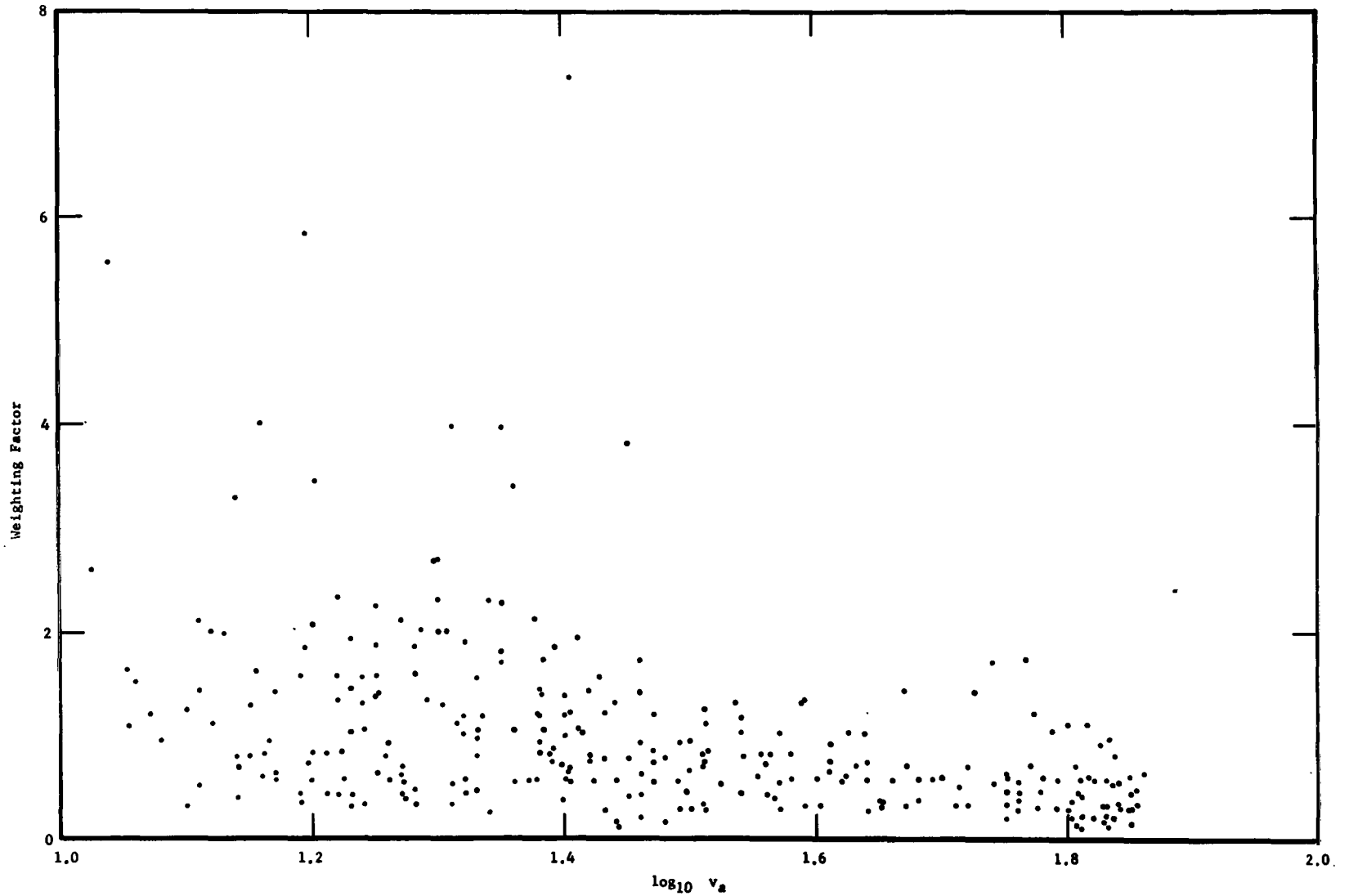

FIGURE 6. VELOCITY-DEPENDENCE OF WEIGHTING FACTORS FOR SPORADIC NOCTURNAL METEORS (REF. 1).

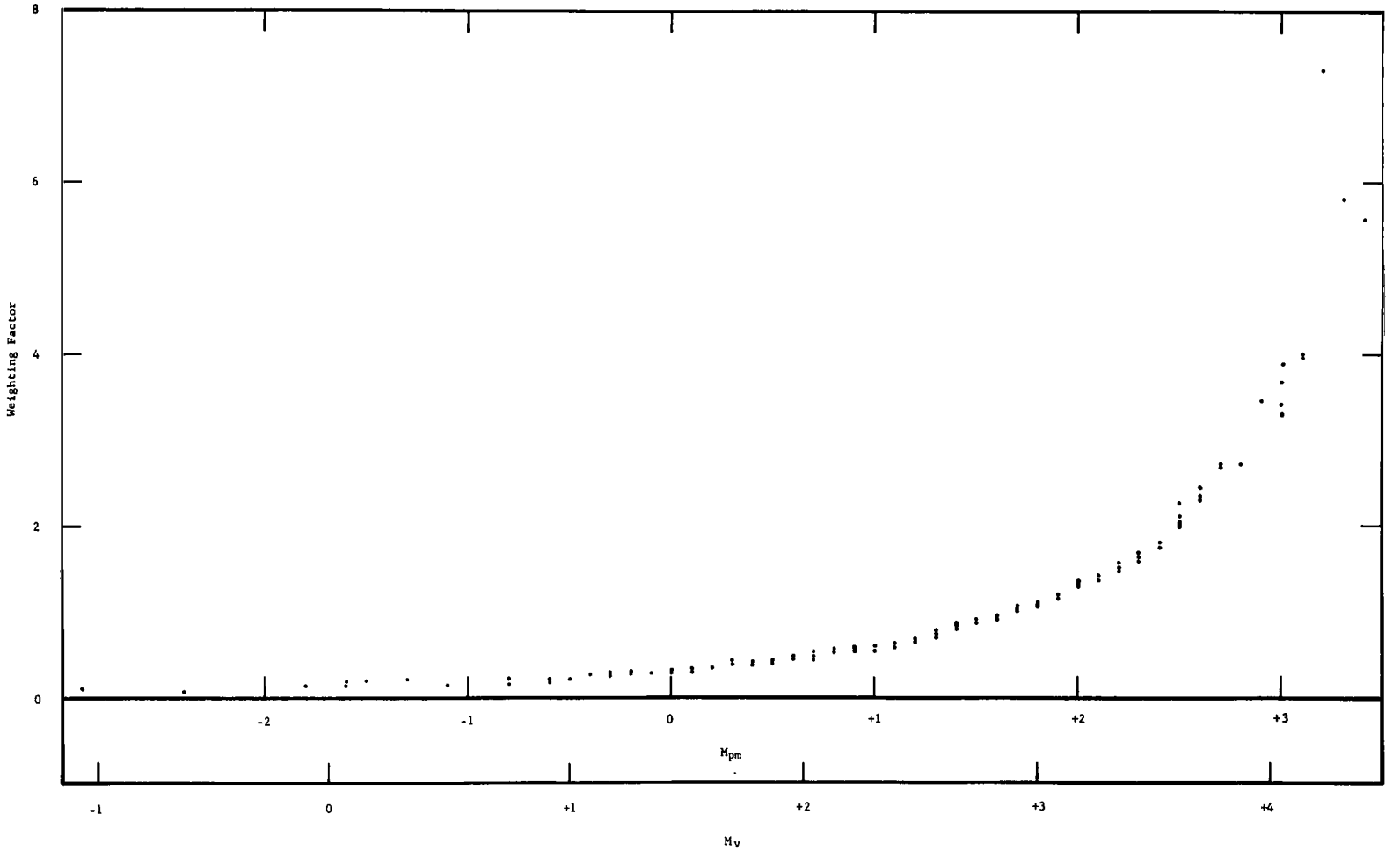

FIGURE 7. MAGNITUDE-DEPENDENCE OF WEIGHTING FACTORS FOR SPORADIC NOCTURNAL METEORS (REF. 1).

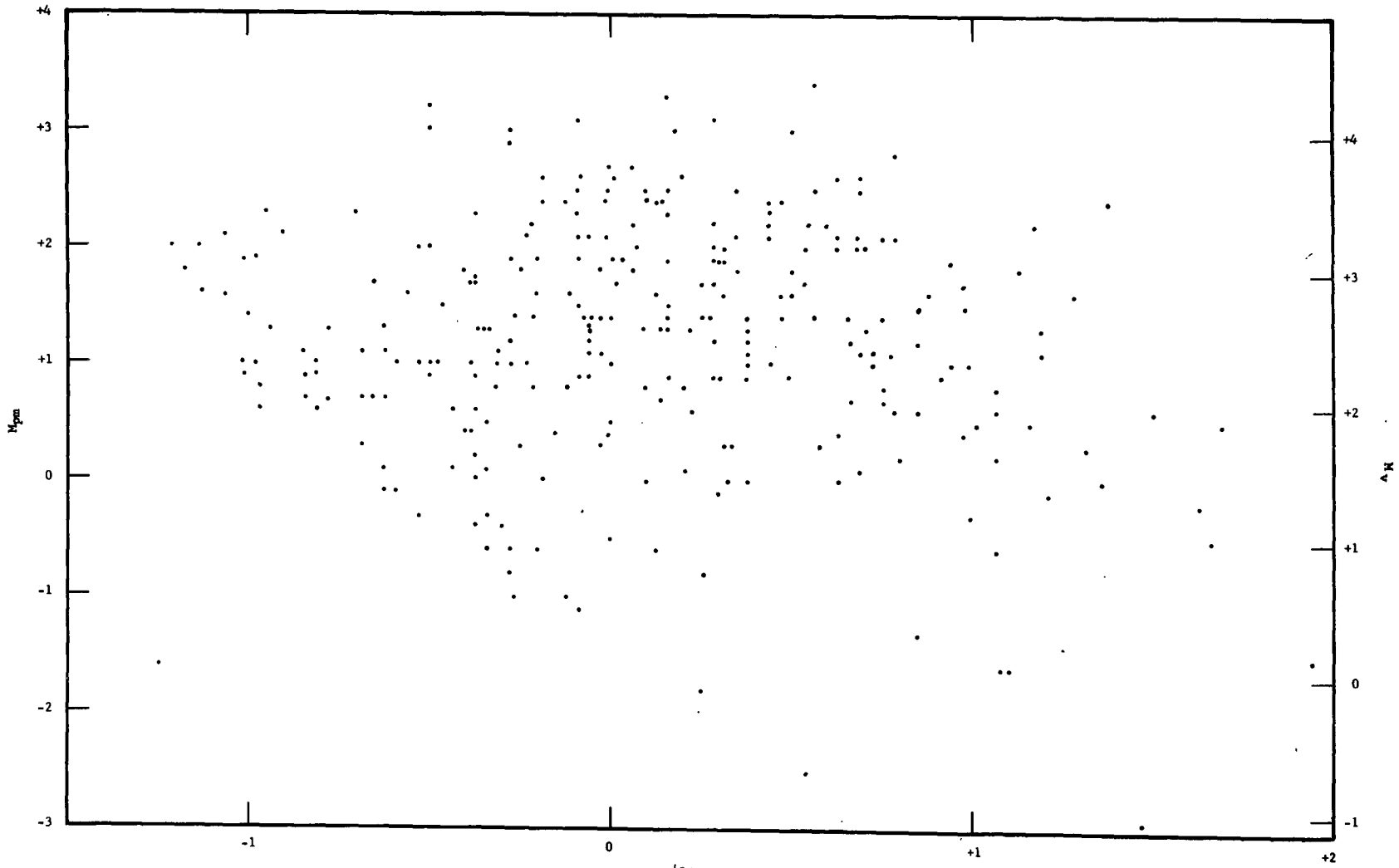

FIGURE 8. MASS-DEPENDENCE OF THE MAGNITUDE OF SPORADIC NOCTURNAL METEORS (REF. 1).

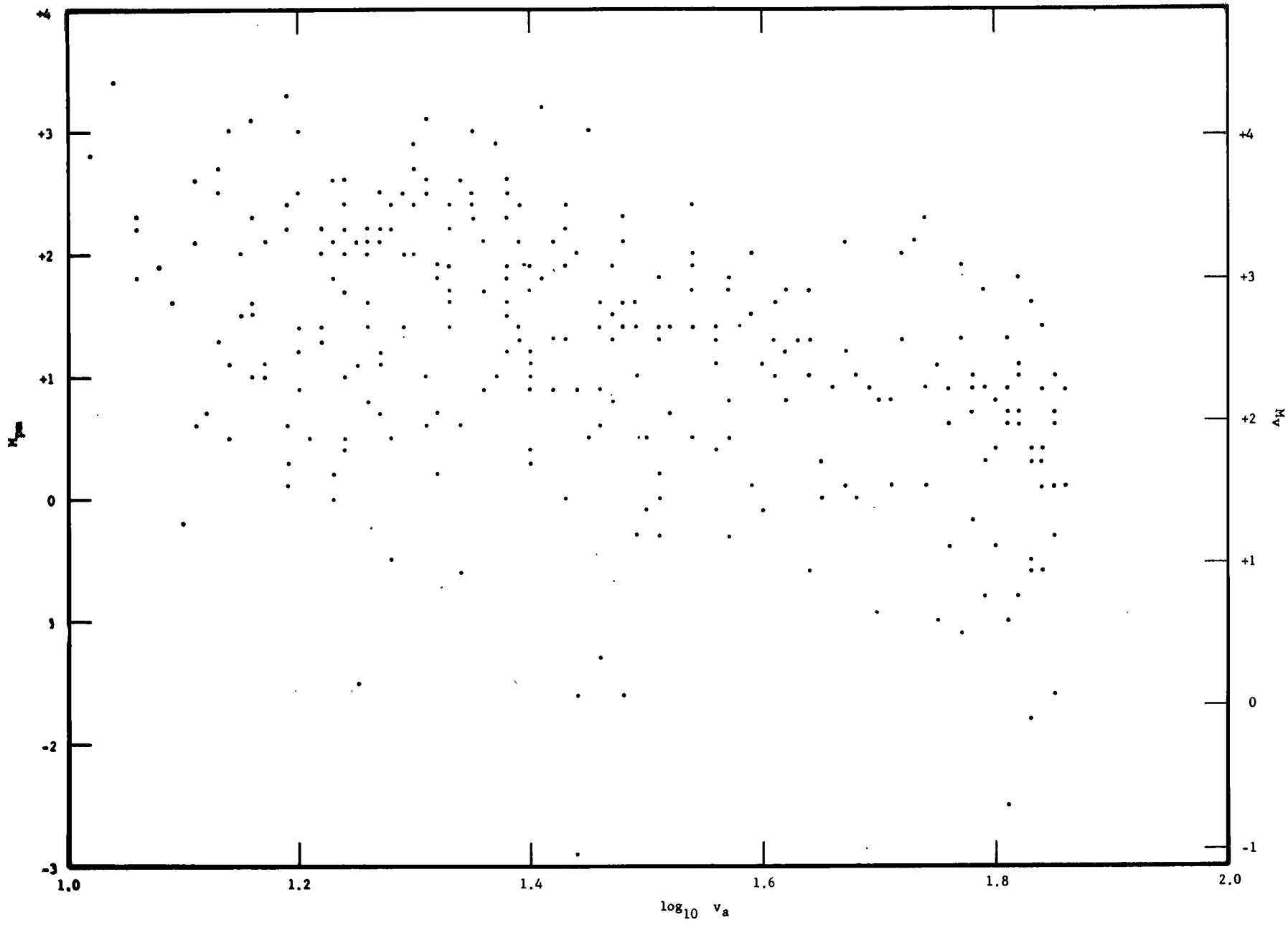

FIGURE 9. VELOCITY-DEPENDENCE OF THE MAGNITUDE OF SPORADIC NOCTURNAL METEORS (REF. 1).

Eq. 4, the mean and standard deviation are

$$E[\log_{10} F_{>}] = \beta_2 \log_{10} m + \beta_3 \tag{30}$$

and

$$\sigma_{\log_{10} F_{>}} = 2\beta_2 \sigma_{y_1} \tag{31}$$

respectively. Therefore, by Eqs. 1, 30, 31, 5, 28, and 29, the tolerance quartiles for the mass dependence of flux are represented by the following formula:

$$\log_{10} F_{>} = -1.42 \log_{10} m - 14.64 \pm 1.92 \tag{32}$$

which is illustrated graphically in Figure 10.

C. METEOROID VELOCITY

1. Relative to the Earth's Atmosphere. Hawkins and Southworth's [1] random sample of 286 nocturnal sporadic meteors in New Mexico (see Section II. B. 2 and II. B. 4) indicates a somewhat surprising relation between velocity v_a and the corresponding values of mass m which were determined in Section II. B. 4. This relation is illustrated in the scatter diagram in Figure 11. It had been expected that the relation could be very well represented by

$$\log_{10} v_a = \beta_4 \log_{10} m + y_2 \tag{33}$$

with β_4 approximately 0.046 and y_2 an approximately normally distributed random variable with mean $\bar{y}_2$ and standard deviation σ_{y_2} approximately 1.51 and 0.12 respectively. But the least-squares solution with uniform weighting gave a linear correlation of -0.82 between $\log_{10} v_a$ and $\log_{10} m$ with the following result:

$$(\beta_4, \bar{y}_2, \sigma_{y_2}) = (-0.30, 1.50, 0.13)$$

Also, by using the non-uniform weighting factors which are described in Appendix A, the least-squares solution gave a linear correlation of -0.82 and also

$$(\beta_4, \bar{y}_2, \sigma_{y_2}) = (-0.31, 1.42, 0.12) \quad .$$

Obviously these results would not be applicable over a very broad range of meteoroid mass in Eq. 33. Therefore, for this analysis, the value for $\bar{y}_2$ is considered to correspond with Whipple's [3] recent estimate of 30 km/sec; i.e., with

$$\beta_4 = 0 \tag{34}$$

and

$$\bar{y}_2 = \log_{10} 30 = 1.48 \tag{35}$$

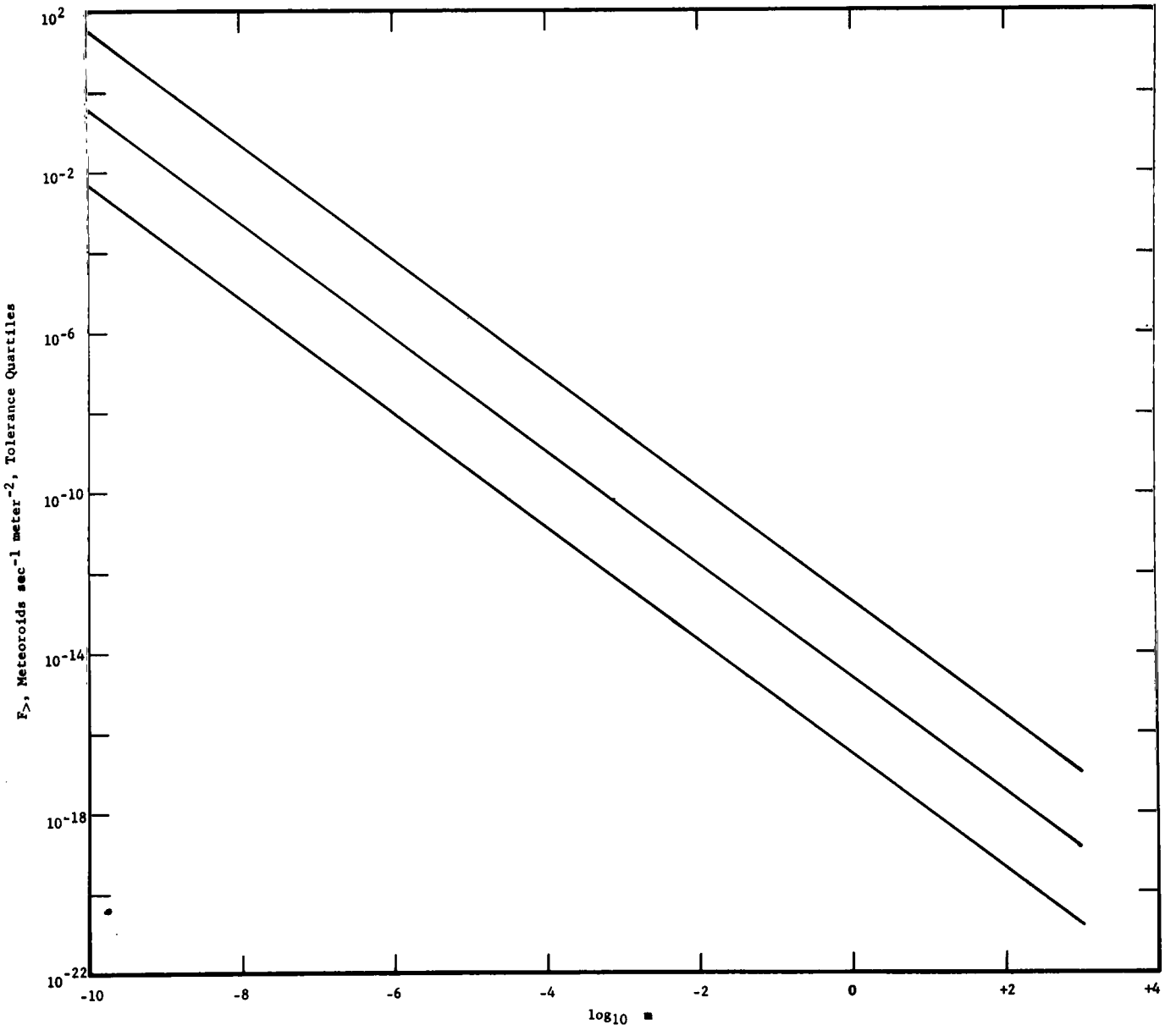

FIGURE 10. MASS-DEPENDENCE OF MEAN ATMOSPHERIC INFLUX OF METEOROIDS WITH MASS ≥ m.

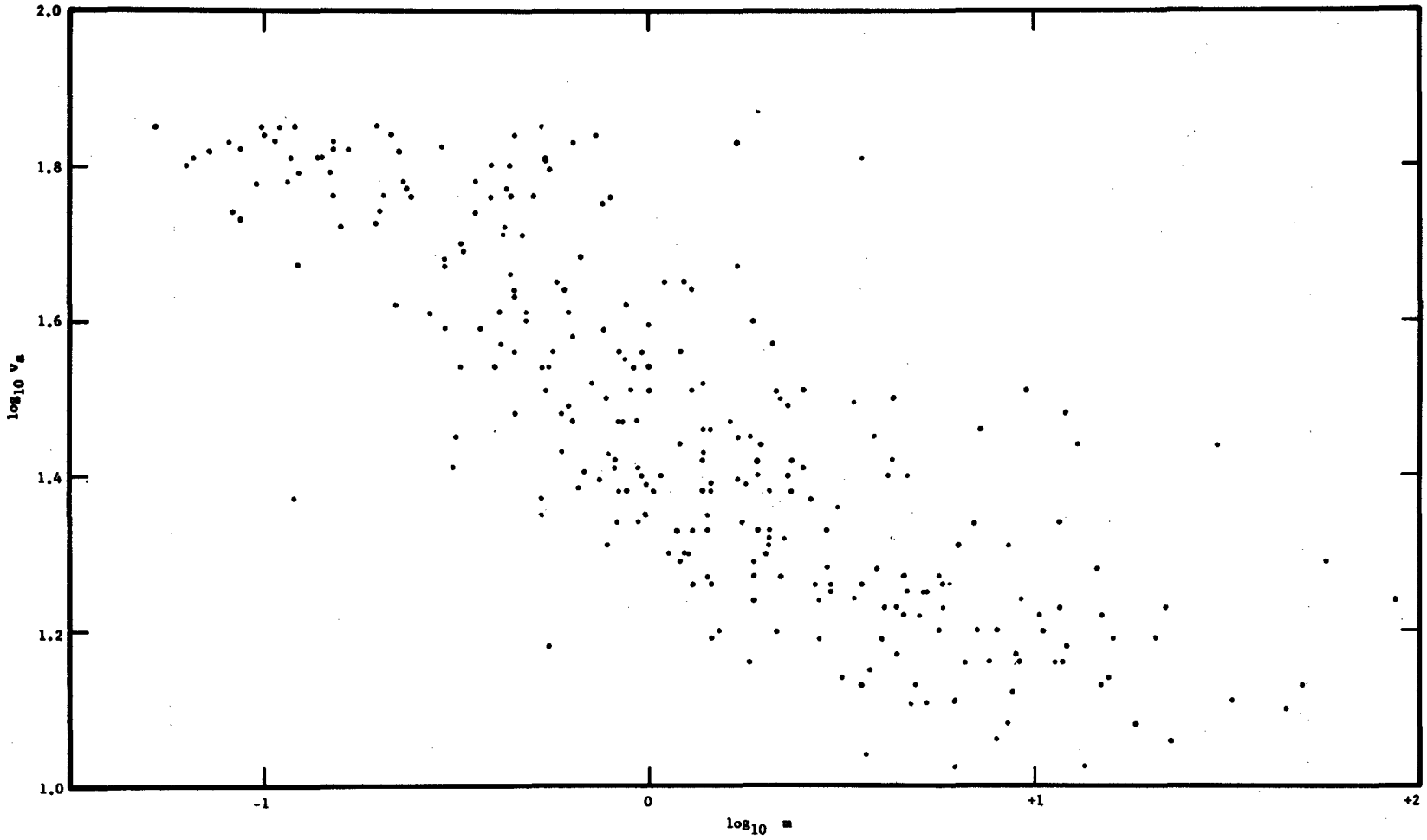

FIGURE 11. MASS-DEPENDENCE OF THE VELOCITY OF SPORADIC NOCTURNAL METEORS (REF. 1).

Also, the standard deviation σ_{y_2} is considered to correspond with a 95% confidence interval of $12.8 \leq v_a \leq 71.2$ km/sec; i.e.,

$$\sigma_{y_2} = 0.19 \tag{36}$$

2. Relative to a Vehicle in Orbit. When a spacecraft is orbiting in a nearly circular orbit with geocentric coordinate r, then its velocity v_s is essentially horizontal with

$$v_s = (\gamma m_e / r)^{\frac{1}{2}} . \tag{37}$$

Then, when one assumes that both the meteoroid and space vehicle are moving in the same plane, the closing velocity v_c is

$$v_c = (v_s^2 + v_r^2 + 2v_r v_s \sin x_1)^{\frac{1}{2}} \tag{38}$$

Because v_r, Eqs. 11 and 38, is always reasonably large with respect to v_s, it is assumed that, just as meteoroid velocity with respect to the Earth's atmosphere can be related to mass by Eqs. 33 and 34, closing velocity v_c with respect to a space vehicle in orbit near the Earth can be similarly related by

$$\log_{10} v_c = y_3 \tag{39}$$

where y_3 is an approximately normally distributed random variable with mean $\bar{y}_3$ and standard deviation σ_{y_3} representing uncertainty of the relation physically and according to available information. Also, because the vehicle is near the Earth, one can substitute r_a for r and v_a for v_r in Eqs. 37 and 38. Therefore, by Eqs. 14 through 16 and 33 through 39,

$$\bar{y}_3 = 1.49 \tag{40}$$

and

$$\sigma_{y_3} = 0.20. \tag{41}$$

D. METEOROID DAMAGE

1. Nature and Function of Material Versus Effects. The meteoroid hazard to space vehicles, or the damage to be expected from meteors, is put in appropriate perspective by the following statement by Rinehart [12] about the concept of quality of failure: "In any particular target, the failure will usually be a complex of many qualities of failure, although frequently a single quality predominates. The basic

problems to consider are what qualities of failure prevail in the situation at hand, which ones are of interest, and whether each quality of failure is an energy-absorbing process, a momentum-absorbing process, or a combination of both. And lastly, what is the quantitative relationship between the extent of failure of a particular quality and the energy and momentum available to cause the failure ··· a few overall qualities of failure are perforation or puncture, volume of crater, volume of failed region, scabbing, spallation, and amount of abrasion..."

The quality of failure which will be emphasized in this report is failure by puncture of a metallic shell. This is necessary to keep the problem from getting too far afield. Should it be expected that the same shell would be more easily punctured when filled with a liquid? Or is it just the other way around? And then, of course, one would want to know what temperature, pressure, shock wave, etc., the liquid is subjected to in the temporal vicinity, what chemical reaction follows, and if there is an explosive vaporization which further rends the structure. But such comprehensive considerations are beyond the scope of this report.

2. Crater Volume in Thick Targets Versus Energy and Momentum for Meteoroids at Normal Incidence. Rinehart [12] illustrates his contention that the volume of the crater produced in a target material by an impacting meteoroid is a linear combination of the kinetic energy ($\frac{1}{2}$ mv_c^2) and momentum (mv_c) of the meteoroid with respect to the target. He says that "...if a failure results from application of an impulse under which the material dislodges easily and offers the inertia of its own mass as a resistance to motion, then the process is a momentum transfer (a flicking away of material, so to speak). On the other hand, if the body steadily continues to resist application of the force, the process is energy-absorbing (pushing of material against a force). Perforation of a thin plate by a projectile, or penetration into a laminated structure such as wood, are momentum-absorbing processes. An energy-absorbing process is the formation of a deep crater in steel by the impact of a heavy projectile. In most real materials, the failure will be a combination of the two."

Both Eichelberger [13] and Beard [8] imply that, for any given target and meteoroid material and structure, crater volume is essentially proportional to kinetic energy ($\frac{1}{2}$ mv_c^2) independently of momentum (mv_c). Eichelberger [13] says "The [empirical] results support very strongly the conclusion from fundamental considerations that cavitation plays the dominant role in crater formation in ductile materials and explains the linear relationship between volume and energy." Beard [8] says "It is most probable that energy considerations of evaporation, rather than momentum effects, dominate the surface interaction of the micrometeorites with a satellite."

3. Crater Depth in Thick Targets Versus Energy, Momentum, and Density of Meteoroids. Typically the various empirical and theoretical formulas for meteoroid crater depth [14] are the product of the cube root of crater volume and the following three factors: (1) The crater-shape factor, (2) the plate-thickness factor, and (3) the

angle-of-incidence factor. Thus, crater depth p_0 is proportional to the 1/3 power of the mass m if crater volume is a linear combination of energy ($\frac{1}{2}$ mv_c^2) and momentum (mv_c). Since Bjork [15] indicates that p_0 is proportional to $(mv_c)^{1/3}$ he is therefore presumably implying that crater volume is proportional to momentum (mv_c) independently of energy ($\frac{1}{2}$ mv_c^2).

An example of a penetration law that does not imply that crater volume is a linear combination of energy and momentum is the law that can be deduced from data which is graphically presented by Hoenig and Ritter [16]; i.e., that the logarithm of penetration depth is linearly related to the logarithm of crater diameter in the same interval of kinetic energy over which they indicate with another graph that crater diameter is proportional to the square root of kinetic energy. In other words, crater depth p_0 is proportional to $m^{1/2}v_c$ for the experiments performed by Partridge at the University of Utah with wax pellets where impact velocity exceeds the velocity of sound in the target material.

But to what must one say that the crater depth is proportional, when so many factors are available from which to choose? Interestingly enough the geometric mean of Hoeing and Ritter's [16] factor $m^{1/2}v_c$, and Bjork's [15] factor, $(mv_c)^{1/3}$ is $(m^{5/4}v_c^2)^{1/3}$, which is very close to Eichelberger's factor $(mv_c^2)^{1/3}$. However, the author feels that neither momentum nor kinetic energy should be inconsequential. He prefers, in the absence of more convincing contrary information, to consider that crater depth, at normal incidence and for given target and meteoroid material and shape, is represented by

$$p_0 \sim m^{\beta_5} v_c^{y_4} \tag{42}$$

where: (1) β_5 is a constant which will be assumed to have the same value,

$$\beta_5 = 1/3 \tag{43}$$

as when crater volume is a linear combination of momentum and energy, and (2) y_4 is an approximately normally distributed random variable, which represents both randomness and uncertainty because of insufficient information. The algebraic mean for y_4 is considered to be the exponent of the geometric mean of the factors $v_c^{1/3}$ and $v_c^{2/3}$, which would represent proportionality of crater volume to momentum and energy, respectively, i.e.,

$$\bar{y}_4 = 1/2 \tag{44}$$

The standard deviation for y_4 is considered to be one third of the difference between the above mentioned exponents 2/3 and 1/3, i.e., $1/3 \leq y_4 \leq 2/3$ at approximately 87 percent confidence:

$$\sigma_{y_4} = 1/9 \tag{45}$$

Herrmann and Jones [14] say: "Data on cratering has been reported by Summers for copper projectiles impacting copper targets at 7,000 and 11,000 ft/sec [2.13 and 3.35 km/sec], and by Kineke for steel discs impacting lead targets at 16,400 ft/sec [5.00 km/sec]. Both experiments noted that the data for oblique impact compared very well with that for normal impact, if penetration versus the normal component of velocity is plotted." This result can be represented by

$$v_{x_2} = v_c \cos x_2 \tag{46}$$

where x_2 is the angle of incidence relative to the normal to the target surface and is therefore a random variable. Presumably this relation, Eq. 46, will also be sufficiently appropriate for meteoroids hitting other metal targets. By Eq. 46 the angle-of-incidence factor by which the right side of Eq. 42 must be multiplied is $(\cos x_2)^{y_4}$, and therefore Eq. 42 is replaced by

$$p_0 \sim m^{1/3} (v_c \cos x_2)^{y_4} \quad . \tag{47}$$

To establish the statistical definition of x_2 in Eq. 47, consider a meteoroid incident on a sphere and an axis parallel to the path of the meteoroid but containing the center of the sphere. The plane normal to the axis and containing the center of the sphere divides the sphere into two hemispheres, and the one which is hit is orthogonally projected onto its base plane. If x_2 is the angle of incidence of the meteoroid relative to the normal to the surface of the hemisphere, then all meteoroids which are parallel to the axis and which will have angles in the interval between x_2 and $x_2 + dx_2$ will be projected onto a ring with radii in the interval between $R \sin x_2$ and $R \sin x_2 + d(R \sin x_2)$. The relative area of the differential ring is the probability density function for angular incidence x_2, i.e., $0 \le x_2 \le \frac{1}{2}\pi$ and

$$f(x_2) = \sin 2x_2 \quad . \tag{48}$$

Since $f(x_2)$ by Eq. 48 is symmetric with respect to $\frac{1}{4}\pi$, it follows that both the mean and median of x_2 are given by

$$\bar{x}_2 = \tfrac{1}{4}\pi \text{ radians.} \tag{49}$$

Then the standard deviation of x_2 is

$$\sigma_{x_2} = (\pi^2/16 - \tfrac{1}{2})^{\frac{1}{2}} = 0.34 \text{ radians.} \tag{50}$$

It is necessary to extend the (Eq. 47) formula for crater depth p_0. The following (Eq. 51) complete formula is established in Appendix C (Eq. 118).

$$p_0 = 10^{1.222 - 0.688 y_4 + y_5} \left(\frac{\rho_p m}{\rho_t H_t}\right)^{\frac{1}{3}} (v_c \cos x_2)^{y_4} \tag{51}$$

where: (1) ρ_t and H_t are the wall density and Brinell Hardness respectively, and (2) y_5 is a random variable which is approximately normally distributed with the following mean $\bar{y}_5$ and standard deviation σ_{y_5} (Eqs. 114 and 115):

$$\bar{y}_5 = -0.44 \tag{52}$$

$$\sigma_{y_5} = 0.08 \quad . \tag{53}$$

The variation of y_5 accounts for the variation of p_0 for impact velocity 4.88 km/sec (16,000 ft/sec) at normal incidence.

4. Thickness of a Just-Puncturable Wall Versus Mass, Density, Velocity, and Angle of Incidence of Meteoroids. The thickness p of a just-puncturable wall is related to the thick-target crater depth p_0 by the target thickness factor 10^{y_6}, i.e.,

$$p/p_0 = 10^{y_6} \tag{54}$$

where y_6 is an approximately normally distributed random variable which represents both the randomness of the process and the uncertainty in the information about it. Bjork's comment is: "The calculations were made for thick targets, but enough information was obtained to deduce that if a projectile penetrates a depth p in a thick target, it will just penetrate a sheet of the same target material which is 1.5p thick." Black [17] says: "To allow a 'bulge' although 'just not perforated', a skin gage of 1.5 times crater depth is generally assumed. (Note that this should be 2 - 3 if the results of Jaffe and Rittenhouse are used)." Eichelberger's [13] "rule of thumb" is that "...a meteoroid...will produce a hemispherical crater of volume τ...if the thickness of the skin is less than $(3\tau/2\pi)^{1/3}$ (or even if it is slightly greater), the skin will be perforated." In other words, the factor is $2^{1/3} = 1.26$ or slightly greater. Herrmann and Jones [14] illustrate experimental results (which they attribute to Kinard et.al. at NASA Langley) and an empirical formula indicating that, as shell thickness is decreased toward the value p, the value of p/p_0 approaches

$$p/p_0 \rightarrow (1/1.3)^2 + 1 = 1.59 \quad . \tag{55}$$

These (Eq. 55) results are said to have been obtained with "...steel and aluminum projectiles into aluminum targets at impact velocities between 5,000 and 13,000 ft/sec" ..., i.e., between 1.5 and 4 km/sec. When C is the confidence that this (Eq. 54) factor is equal to or less than the stated value, then it seems appropriate that the above mentioned four estimates should be accepted as follows:

$$(C,\ 10^{y_6}) = (0.16,\ 1.26),\ (0.41,\ 1.50),\ (0.50,\ 1.59),\ (0.976,\ 2.5) \tag{56}$$

$$\bar{y}_6 = 0.20 \tag{57}$$

$$\sigma_{y_6} = 0.10 \quad . \tag{58}$$

SECTION III. DESIGN AND OPERATIONAL PARAMETERS

A. JUST-PUNCTURABLE METEOROID MASS VERSUS THICKNESS, DENSITY, AND HARDNESS OF THE WALL OF A VEHICLE

By taking the product of Eqs. 51 and 54 and substituting Eqs. 39 and 3 expressions for $\log_{10} v_c$ and $\log_{10} \rho_p$, one finds that meteoroid mass m in grams and puncturable wall thickness p in centimeters are functionally related as follows:

$$p = 10^{y_7} \left(m/\rho_t H_t\right)^{\frac{1}{3}} \tag{59}$$

where

$$y_7 = y_8 + x_4, \tag{60}$$

where

$$y_8 = 1.222 + 0.333\, y_1 + y_5 + y_6, \tag{61}$$

and

$$x_4 = y_4 x_5 \tag{62}$$

where

$$x_5 = -0.688 + y_3 + x_6, \tag{63}$$

where

$$x_6 = \log_{10} \cos x_2 \quad . \tag{64}$$

With the probability density function for angle of impact x_2 in Eq. 48 it follows that the mean $\overline{x}_6$ and variance $\sigma^2_{x_6}$ of the random variable x_6 in Eq. 64 are:

$$\overline{x}_6 = \int_0^{\pi/2} (\log_{10} \cos x_2)\, \sin 2x_2\, dx_2 = -\tfrac{1}{2} \log_{10} e = -0.22 \tag{65}$$

$$\sigma^2_{x_6} = \int_0^{\pi/2} (\log_{10} \cos x_2 + \tfrac{1}{2} \log_{10} e)^2 \sin 2x_2\, dx_2 = \tfrac{1}{4} (\log_{10} e)^2 = 0.047 \tag{66}$$

Because the means and variances are additive for the sum of statistically independent

random variables, it follows from the numerical values for $\overline{y}_3$, σ_{y_3}, $\overline{x}_6$, and σ_{x_6} in Eqs. 40, 41, 65 and 66, respectively, that the mean $\overline{x}_5$ and variance $\sigma^2_{x_5}$ of the random variable x_5 in Eq. 63 are:

$$\overline{x}_5 = -0.688 + \overline{y}_3 + \overline{x}_6 = 0.58 \tag{67}$$

$$\sigma^2_{x_5} = \sigma^2_{y_3} + \sigma^2_{x_6} = (0.20)^2 + (0.22)^2 = 0.088 = (0.30)^2 \quad . \tag{68}$$

Because the mean of the product of statistically independent random variables is the product of the means, it follows from the numerical values for $\overline{y}_4$ and $\overline{x}_5$ in Eqs. 44 and 67, respectively, that the mean $\overline{x}_4$ of the random variable x_4 in Eq. 62 is

$$\overline{x}_4 = \overline{y}_4\,\overline{x}_5 = 0.29 \quad . \tag{69}$$

When x_4 is approximated by the linear part of the Taylor series expansion of the product $y_4\,x_5$, it follows from the numerical values for $\overline{y}_4$, σ_{y_4}, $\overline{x}_5$, and σ_{x_5} in Eqs. 44, 45, 67, and 68, respectively, that the variance $\sigma^2_{x_4}$ is

$$\sigma^2_{x_4} = \left(\frac{\partial x_4}{\partial y_4}\,\sigma_{y_4}\right)^2 + \left(\frac{\partial x_4}{\partial x_5}\,\sigma_{x_5}\right)^2 = (\overline{x}_5\,\sigma_{y_4})^2 + (\overline{y}_4\,\sigma_{x_5})^2 = 0.026 \quad . \tag{70}$$

The random variable y_8 in Eq. 61 is a linear combination of statistically independent normal random variables and is therefore also normal. With the numerical values for $\overline{y}_1$, σ_{y_1}, $\overline{y}_5$, σ_{y_5}, $\overline{y}_6$, and σ_{y_6} in Eqs. 4, 5, 52, 53, 57, and 58, respectively, and the coefficients in Eq. 61, it follows that y_8 has the following mean $\overline{y}_8$ and variance $\sigma^2_{y_8}$:

$$\overline{y}_8 = 1.222 + 0.333\,\overline{y}_1 + \overline{y}_5 + \overline{y}_6 = 0.86 \tag{71}$$

$$\sigma^2_{y_8} = (0.333\,\sigma_{y_1})^2 + \sigma^2_{y_5} + \sigma^2_{y_6} = 0.128 \quad . \tag{72}$$

Because y_7 in Eq. 60 is a linear combination of the statistically independent random variables y_8 and x_4, it follows with the values of $\overline{x}_4$, σ_{x_4}, $\overline{y}_8$, and σ_{y_8} in Eqs. 69 through 72, respectively, that the mean $\overline{y}_7$ and variance $\sigma^2_{y_7}$ are

$$\overline{y}_7 = \overline{y}_8 + \overline{x}_4 = 1.15 \tag{73}$$

and

$$\sigma^2_{y_7} = \sigma^2_{y_8} + \sigma^2_{x_4} = 0.154 = (0.39)^2 \quad . \tag{74}$$

By the ratio of Eqs. 72 and 74, 83 percent of the variance of y_7 is due to the normal variable y_8. Therefore the facts that the smaller component of the variance in y_7 is

only a first order approximation and that the variable which contributes that smaller variance is not normally distributed can be ignored without appreciable error. Then y_7 in Eq. 59 is approximately normally distributed with mean and probable error expressed by

$$y_7 = \overline{y}_7 \pm 0.6745\, \sigma_{y_7} = 1.15 \pm 0.26 \quad . \tag{75}$$

Therefore, by Eqs. 59 and 75, the wall thickness tolerance quartiles for the puncturability of p centimeters by a meteoroid of mass m grams can be represented by

$$p = 10^{1.15 \pm 0.26}\, (m/\rho_t H_t)^{\frac{1}{3}} \tag{76}$$

These results (Eq. 76) are represented graphically in Figures 12 and 13 for the following two respective metallic walls:

$$(\rho_t, H_t) = (2.80, 135): \text{ hard alluminum alloy} \tag{77}$$

$$= (7.42, 310): \text{ hard stainless steel} \tag{78}$$

B. METEOROID PUNCTURE-FLUX VERSUS THICKNESS, DENSITY, AND HARDNESS OF THE WALL OF A VEHICLE

The puncture flux ϕ is that value of $F_>$ in Eq. 23 corresponding to a just-puncturable value of m. The following formula is obtained by substituting into Eq. 23 the expression for $\log_{10} m$ from Eq. 59 and the expression for ρ_p from Eq. 3; i.e.,

$$\phi = 10^{y_9} (\rho_t H_t p^3)^{\beta_2} \tag{79}$$

where

$$y_9 = \beta_3 + 2\beta_2 \log_{10}\beta_1 - \beta_2 (3y_7 + 2y_1) \quad . \tag{80}$$

By Eqs. 60 and 61 the last term in Eq. 80 is

$$-\beta_2 (3y_7 + 2y_1) = -3\beta_2 (1.222 + y_1 + y_5 + y_6 + x_4) . \tag{81}$$

Therefore, with the values for β_1, β_2, and β_3 from Eqs. 2, 28, and 29, respectively, Eq. 80 becomes

$$y_9 = -8.43 + 4.26\, (y_1 + y_5 + y_6 + x_4) \tag{82}$$

Then, with the means $\overline{y}_1$, $\overline{y}_5$, $\overline{y}_6$, and $\overline{x}_4$ from Eqs. 4, 52, 57, and 69, respectively, the mean $\overline{y}_9$ is

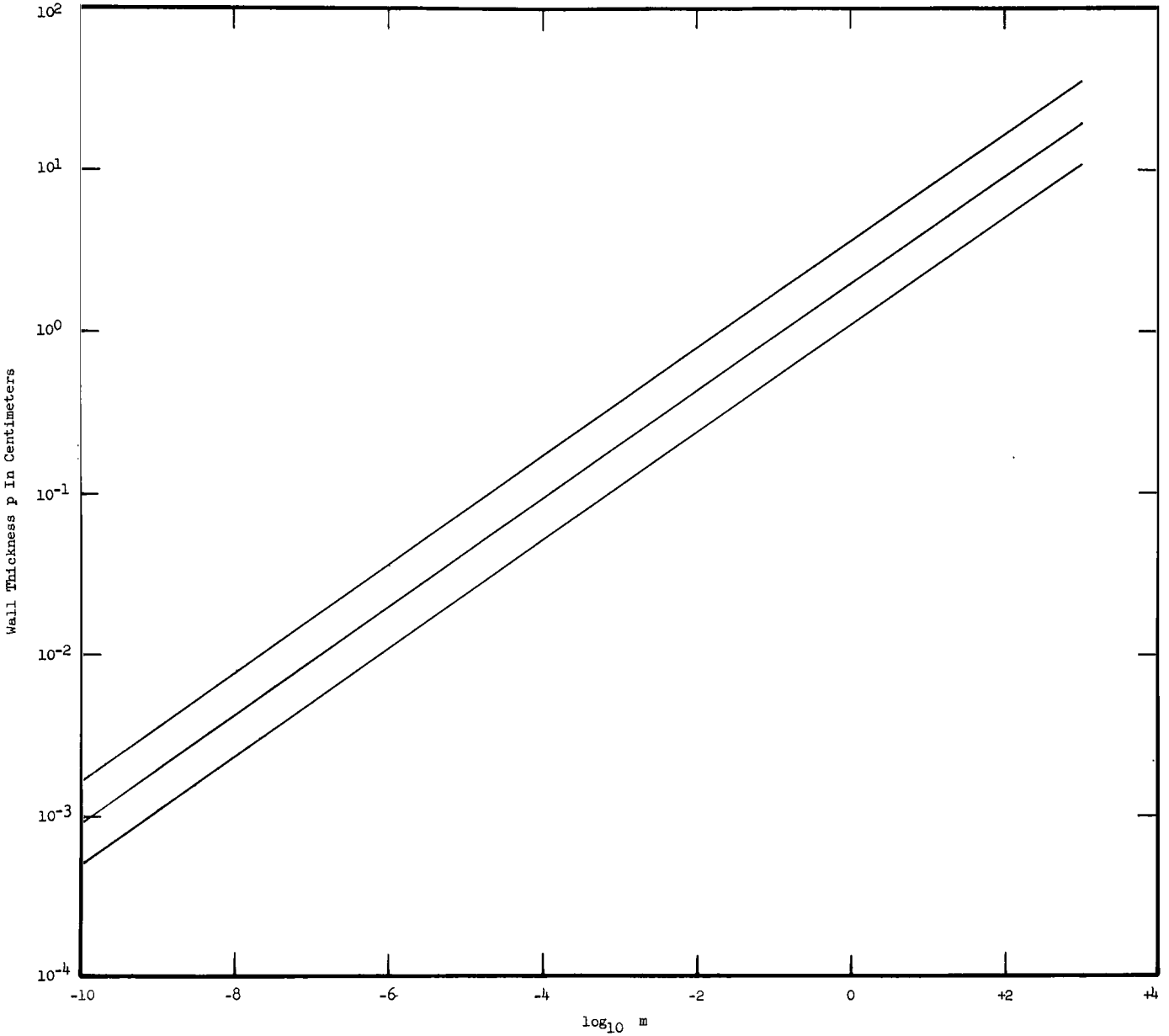

FIGURE 12. QUARTILES FOR THE THICKNESS OF A WALL OF HARD ALUMINUM ALLOY JUST PUNCTURABLE BY A METEOROID OF MASS m (GRAMS).

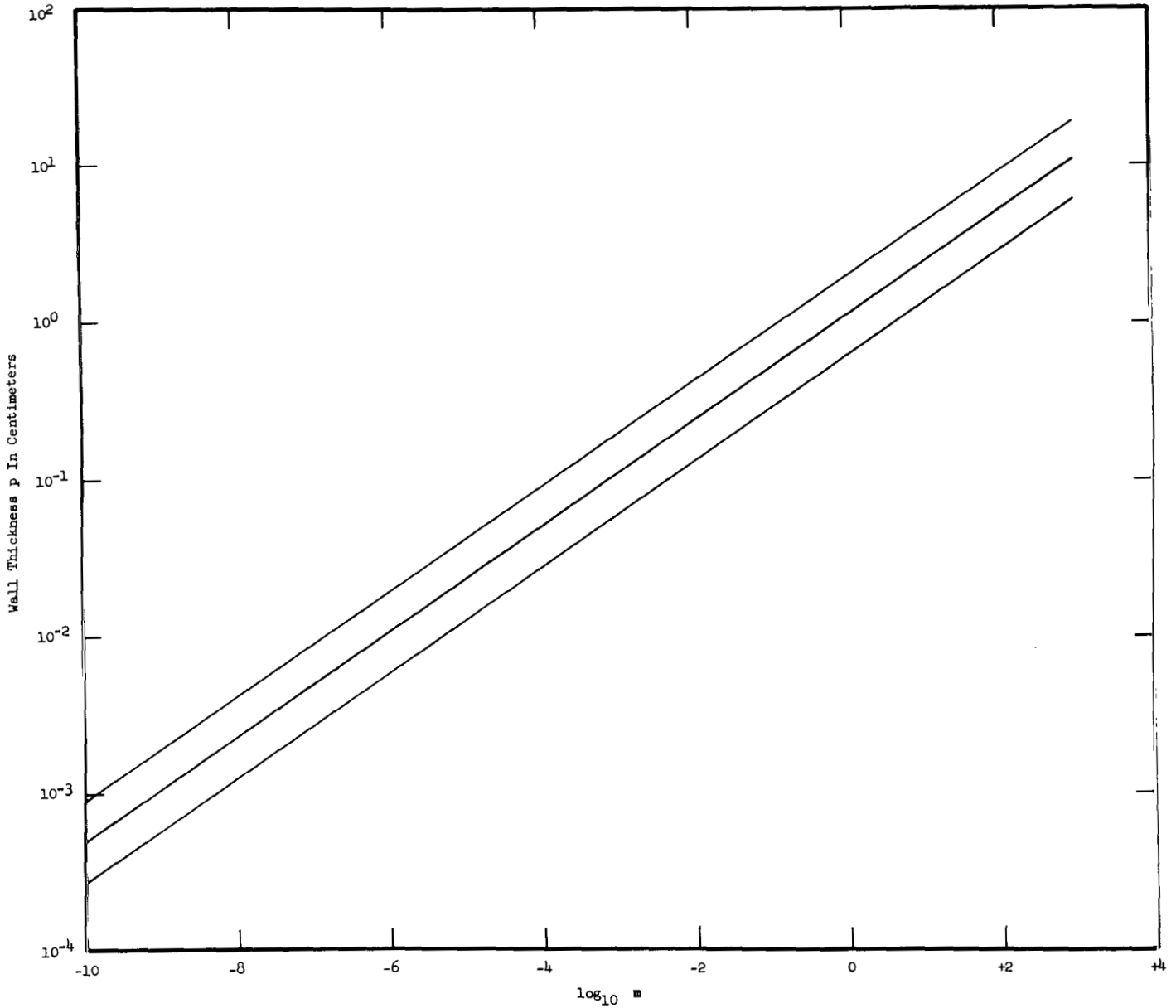

FIGURE 13. QUARTILES FOR THE THICKNESS OF A WALL OF HARD STAINLESS STEEL JUST PUNCTURABLE BY A METEOROID OF MASS m (GRAMS).

$$\bar{y}_9 = -8.43 + 4.26\,(\bar{y}_1 + \bar{y}_5 + \bar{y}_6 + \bar{x}_4) = -9.73 \quad . \tag{83}$$

With the values of the standard deviations in Eqs. 5, 53, 58, and 70 it follows that the variable x_4 contributes only $2\frac{1}{2}$ percent of the variance of y_9; i.e.,

$$\sigma^2_{x_4} / (\sigma^2_{y_1} + \sigma^2_{y_5} + \sigma^2_{y_6} + \sigma^2_{x_4}) = 0.025 \quad . \tag{84}$$

Therefore no appreciable error is introduced by using the first order approximation for σ_{x_4} in Eq. 70 and considering y_9 in Eqs. 82 to be approximately normally distributed with standard deviation σ_{y_9} given by

$$\sigma_{y_9} = 4.26\,(\sigma^2_{y_1} + \sigma^2_{y_5} + \sigma^2_{y_6} + \sigma^2_{x_4})^{\frac{1}{2}} = 4.35 \quad . \tag{85}$$

Then the mean and probable error for the exponent of the puncture flux coefficient can be expressed by

$$y_9 = \bar{y}_9 \pm 0.6745\,\sigma_{y_9} = -9.73 \pm 2.93 \tag{86}$$

Consequently, by Eqs. 28, 79, 86, the meteoroid puncture flux tolerance quartiles for wall thickness p can be represented by

$$\phi = 10^{-9.73 \pm 2.93}\,(\rho_t H_t p^3)^{-1.42} \quad . \tag{87}$$

These results (Eq. 87) are represented graphically in Figures 14 and 15 for walls of hard aluminum and hard stainless steel specified by Eqs. 77 and 78 respectively.

C. WALL THICKNESS VERSUS THE PRODUCT OF EXPOSED AREA AND DURATION FOR GIVEN PROBABILITIES OF NO PUNCTURE

By substituting the (Eq. 79) expression for ϕ into the (Eq. 8) expression for no-puncture probability R, and taking the common logarithm of the natural logarithm of both sides of the resulting expression, one finds

$$\log_{10}(-\log_e R) = \log_{10} At\,(\rho_t H_t)^{\beta_2} + 3\beta_2 \log_{10} p + y_9 \quad . \tag{88}$$

Eq. 88 can be solved for $\log_{10} p$ as a linear function of the normal random variable y_9. Then, with the values of β_2, $\bar{y}_9$, and σ_{y_9} from Eqs. 28, 83, and 85, respectively, the mean and probable error of $\log_{10} p$ can be expressed by

$$\log_{10} p = -0.235\,[\log_{10}(-\log_e R) - \log_{10} At] - 0.333 \log_{10} \rho_t H_t - 2.29 \pm 0.69 \tag{89}$$

$$= E[\log_{10} p] \pm 0.69 \quad . \tag{90}$$

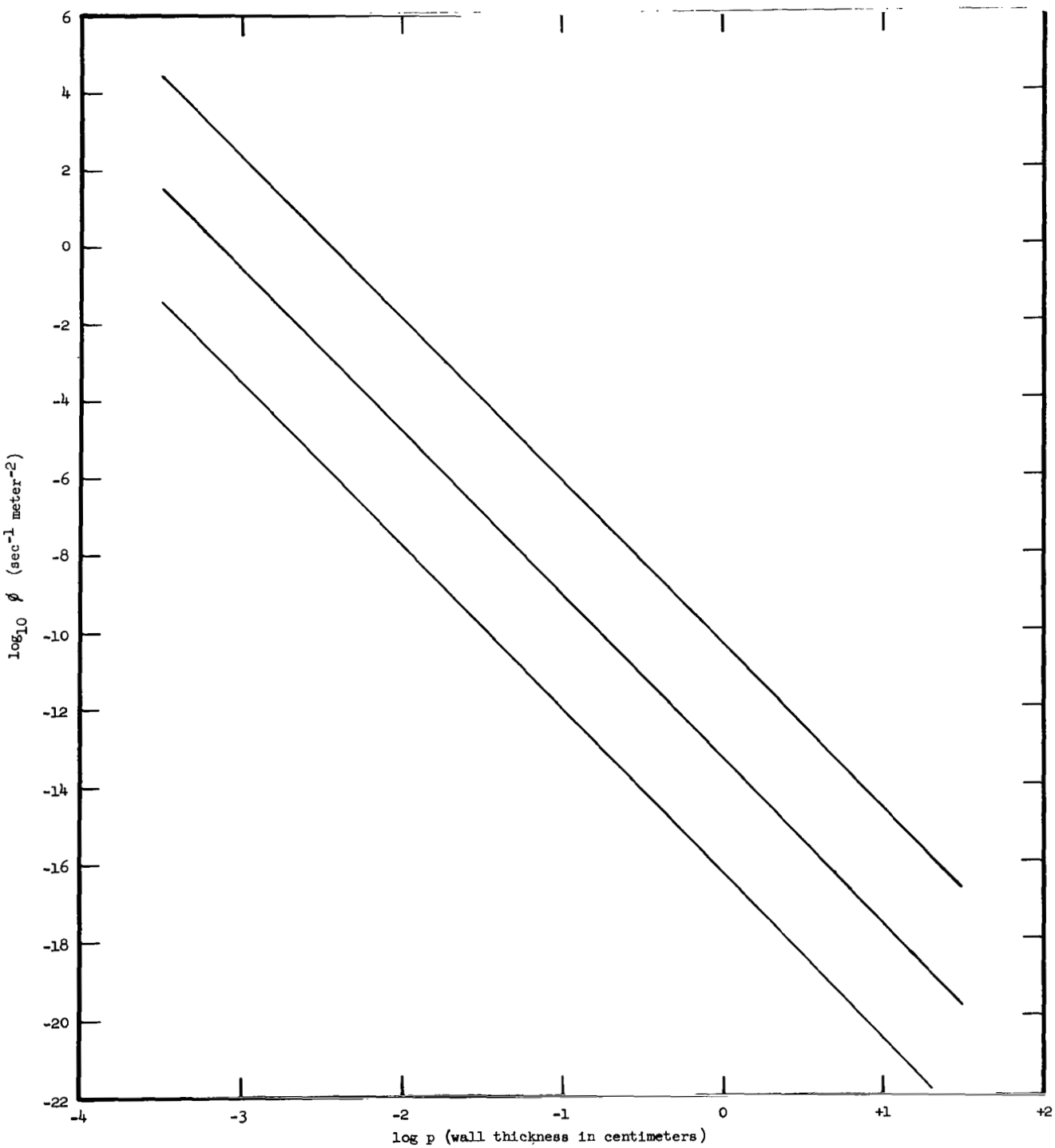

FIGURE 14. QUARTILES FOR METEOROID PUNCTURE FLUX FOR A WALL OF HARD ALLUMINUM ALLOY.

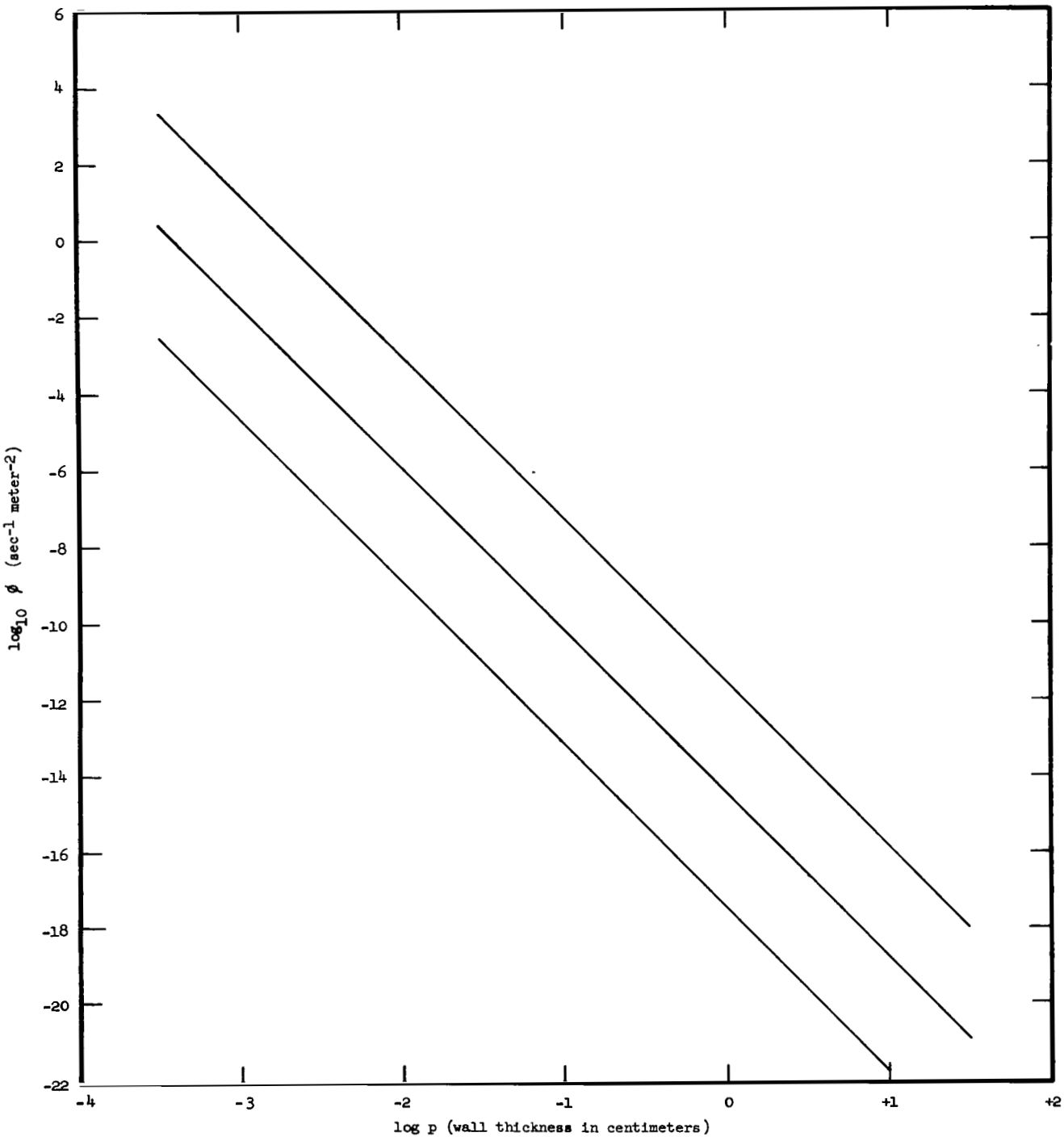

FIGURE 15. QUARTILES FOR METEOROID PUNCTURE FLUX FOR A WALL OF HARD STAINLESS STEEL.

Therefore, the wall thickness tolerance quartiles can be represented by

$$p = 10^{E[\log_{10} p] \pm 0.69} . \tag{91}$$

D. AMELIORATING CONSIDERATIONS

Nysmith and Summers [2] reported that a two-sheet wall structure with a sheet spacing of one inch with interspersed glass wool filler has about 4.4 times greater penetration resistance than a single sheet of material of the same total-sheet thickness.

SECTION IV. CONCLUSIONS

Present information about meteoroids and their puncturability is so poor that there is only an even chance that mean puncture flux (for a single sheet of specified metal of specified thickness) is between upper and lower limits which are separated by almost six orders of magnitude. And if a vehicle has been designed so that for a specified mission there is only one chance in two that the no-puncture probability is less than a specified value, then it is necessary to increase the wall thickness by a factor of almost five so that the chance is reduced to only one in four that the no-puncture probability is less than the same specified value. It is expected that further information will become available from time to time as space technology continues to develop through analysis, experimentation, and experience. Therefore, the latest available information should be considered for specific purposes.

APPENDIX A. NON-UNIFORM WEIGHTING FOR METEOR DATA

A random sample of photographic meteor data does not quite represent a random sample of nocturnal meteoroids when uniform weighting is assumed, because meteors of larger absolute magnitude are detectable over an appreciably smaller area. The resulting bias should be considerably reduced by weighting the i^{th} datum (where $i = 1, 2, \ldots, n_t$) with the relative value of the reciprocal of the area A_i over which the meteor, of the same absolute visual magnitude M_{V_i} and height in kilometers h_i at maximum brilliance, could have been assessed. Then the weighting factor for the i^{th} datum is

$$f_i = n_t A_i^{-1} / \sum_{i=1}^{n_t} A_i^{-1} \tag{92}$$

$$A_i = \pi [(6378 + h) \sin \theta_i]^2 \tag{93}$$

Where 6378 is the radius of the Earth in kilometers and where θ_i would be the geocentric angular separation of the station and the meteor at maximum brilliance beyond which there would not have been effective assessment. An appropriate expression for $\sin \theta$ in Eq. 93 can be found from the following relation:

$$[(6378 + h_i) \cos \theta_i - 6378] \tan Z_i = (6378 + h_i) \sin \theta_i \tag{94}$$

where Z_i would be the angle between the station zenith and the meteor with geocentric coordinate θ_i; i.e.,

$$\sin \theta_i = \left[\left(\frac{6378}{6378 + h_i}\right) \sin Z_i\right]\left[\sqrt{\left(\frac{6378 + h_i}{6378}\right)^2 - \sin^2 Z_i} - \cos Z_i\right] . \tag{95}$$

Absolute visual magnitude M_{V_i} of a meteor is the magnitude it would have if it were placed in the zenith at a standard range of 100 kilometers. It is related to the equipment-limiting apparent visual magnitude M by

$$M_{V_i} = M - \Delta M_i - 5 \log_{10} [10^{-2} (6378 + h_i) \sin \theta_i \csc Z_i] \tag{96}$$

where ΔM_i is an adjustment for atmospheric absorption. McKinley [18] indicates that, according to the Handbuch der Astrophysik, ΔM_i in the interval $0 \leq \Delta M_i \leq 3.2$ is linearly related to sec Z_i in the interval $1 \leq \sec Z_i \leq 10$; i.e., that

$$\Delta M_i = 0.36 (\sec Z_i - 1) \tag{97}$$

The relation between absolute visual magnitude M_{v_i} and absolute photographic magnitude M_{pm_i} is given by Eq. 26 in Section II. A. 4. Therefore, by Eqs. 26 and 95 through 97, Z_i in Eq. 95 must satisfy the following equation:

$$M - 10.11 - 0.86\, M_{pm_i} = 0.36 \sec Z_i + 5 \log_{10}\left[\sqrt{\left(\frac{6378 + h_i}{6378}\right)^2 - \sin^2 Z_i} - \cos Z_i\right] \tag{98}$$

$$= 0.36 \sec Z_{0_i} + 5 \log_{10}\left[\sqrt{\left(\frac{6378 + h_{0_i}}{6378}\right)^2 - \sin^2 Z_{0_i}} - \cos Z_{0_i}\right] \tag{99}$$

where M is replaced by the equipment limiting apparent visual magnitude sensitivity, where h_{0_i} is the middle of the class interval which contains h_i and where Z_{0_i} is the value of Z which would very nearly correspond to h_{0_i}. With large samples it is not convenient to solve Eq. 98 directly for each datum. It is more appropriate to consider four class intervals ($h < 80$, $80 \leq h < 90$, $90 \leq h < 100$, and $h > 100$) and calculate a set of values of the right side of Eq. 99 for each class at increments of $\pi/200$ for $0 < Z_0 < \pi/2$. Then for each of the n_t values of the left side of the equation, the right side is scanned by trial subtraction and the difference changes sign at some least near-solution Z_{0_i}. The relation between Z_i and Z_{0_i} is then found by approximating the ratio of the increments of Z and h by the negative of the inverse ratio of the partial derivatives of the difference between the right sides of Eqs. 98 and 99. In that way, because $(5/0.36) \log_{10} e = 6.0$, it can be shown that:

$$Z_i = Z_{0i} - \frac{6\left(\frac{h_i - h_{0_i}}{6378}\right)\left(\frac{6378 + h_i}{6378}\right) \cos^2 Z_{0i} \csc Z_{0i}}{\left[\sqrt{\left(\frac{6378 + h_i}{6378}\right)^2 - \sin^2 Z_{0i}} - \cos Z_{0i}\right]\left[\sqrt{\left(\frac{6378 + h_i}{6378}\right)^2 - \sin^2 Z_{0i}} + 6\cos^2 Z_{0i}\right]} \tag{100}$$

In evaluating the weighting factors f_i in Eq. 92, the factor $\pi(6378)^2$ is common to each A_i. Therefore, by Eqs. 93 and 95, what one needs in Eq. 92 is the following result for each meteor:

$$\pi(6378)^2 A_i^{-1} = \left\{\left[\sqrt{\left(\frac{6378 + h_i}{6378}\right)^2 - \sin^2 Z_i} - \cos Z_i\right] \sin Z_i\right\}^{-2} . \tag{101}$$

This method of non-uniform weighting, when applied to the random sample of 286 sporadic photographic meteor data by Hawkins and Southworth [1] discussed in Sections II. A. 2, II. A. 4, and II. B. 1, gives the results which are illustrated graphically in Figures 2, and 4 through 7.

APPENDIX B. METHOD FOR RELATING SAMPLE VALUES OF METEOR PARAMETERS AND THE APPROXIMATE ONE-SIDED TOLERANCE QUARTILE VALUES FOR THEIR CUMULATIVE PROBABILITY.

When the probability density function is known, for the population of values of a parameter from which one has a representative sample of size n_t, one can express any percentile (tolerance or confidence limit) for the cumulative probability of the population at any partitioning value of the parameter as a function of the sample moments. But, with state of the art meteor and meteoroid technology, the necessary function to use with photographic meteor data is in doubt to the extent that it seems more appropriate to partition the parameter at the sample values and to assume that the corresponding population cumulative probabilities are the same as one would infer binomially from the number of sample values which exceed the partition in n_t trials.

Some inherent difficulties are involved in this approach which are practically overcome by an approximate method which has not been previously reported. This method is of sufficient general interest for application to a variety of problems that its presentation is given in this technical appendix.

One wants to derive a convenient and sufficiently approximate formula relating p_s explicitly to C, n_f, and n_t where n_f is the number of times an event has occurred during n_t independent trials and C is the cumulative probability or confidence that the probability of event occurrence per trial is not greater than p_s.

When p_s has either a Poisson or a binomial distribution, a convenient approximation to p_s is p_n, where p_n is normally distributed with the following mean $\overline{p}_n$ and standard deviation σ_{p_n}:

$$\overline{p}_n = n_f/n_t \tag{102}$$

$$\sigma_{p_n} = \sqrt{\overline{p}_n (1 - \overline{p}_n)/n_t} \tag{103}$$

Percentiles of orders 0.25, 0.50, and 0.75 for p_n are given for sample size $n_t = 286$ at each value of n_f in the interval $1 \leq n_f \leq 35$ in Table II.

The accuracy of p_n as an approximation to p_s can be examined by substituting for p_s the quartile values of p_n into the following explicit formula for one-sided binomial confidence limits (see reference works on statistical methods; e.g., Lloyd and Lipow's [19])

$$C = 1 - \sum_{i=1}^{n_f} \binom{n_t}{i} p_s^{\,i} (1 - p_s)^{n_t - i} \tag{104}$$

The corresponding values of C are also given for each value of n_f in Table II. Because p_n is a percentile of order C for p_s, disagreement between values of C and the corresponding orders 0.25, 0.50, and 0.75 of the percentiles for p_n indicates that p_n is not a very accurate approximation for p_s when $n_t = 286$ and $1 \leq n_f \leq 35$.

The derivation of the following approximation formula, based on the Poisson failure distribution and other criteria from sequential analysis, was previously reported.

$$p_s = 1 - [(1 - C)/e^{n_f}]^{1/(n_t - n_f/2)} \tag{105}$$

where

$$C \geq 1/2 \tag{106}$$

and

$$n_f \leq n_t/2 \quad . \tag{107}$$

In preparation for the present analysis the author compared the results from Eq. 105 with some results from Eq. 104, for binomial failure distribution, illustrated graphically by Lloyd and Lipow [19]. It was found that, within the reading accuracy of the graph, the two sets of values agreed: (1) for all C when $n_f = 0$, (2) for all n_f when $C = 1/2$, and (3) for all other combinations of n_f and C when the exponent in Eq. 105 is multiplied by the factor $(3+2C)/4$. Therefore it was thought that Eq. 105 is an appropriate approximation for Poisson failure distribution and that a similar approximation for binomial failure distribution is

$$p_s = 1 - [(1 - C)/e^{n_f}]^{[(3+2C)/4]^{\delta}/(n_t - n_f/2)} \tag{108}$$

where

$\delta = 0$ when $n_f = 0$

$= 1$ when $n_f \neq 0$

and C and n_f satisfy Eqs. 106 and 107 respectively. But, by the further results for various combinations of n_f and n_t which are compiled in Table I, one finds that Eq. 108

gives results which are generally intermediate between the corresponding values from Poisson and binomial tables, and that even the Poisson results are as accurately approximated by Eq. 108 as by Eq. 105.

All of the values of $1 - p_s$ shown in Table I are for $C = 0.975$ because that is the value of C for which there are results for the Poisson distribution tabulated by Pearson and Hartley [20] which correspond to values for the binomial distribution tabulated by Hald [21].

Having established, by inspection of Table I, that Eq. 108 may be a reasonably accurate approximation for p_s, the accuracy of the approximations for the percentiles of orders 0.25, 0.50, and 0.75 for p_s is illustrated in Table II in the same manner as has already been described for the normal approximation p_n.

It can be seen in Table II that the values of p_s from Eq. 108 differ substantially from those for the normal approximation p_n for each quartile and for each value of n_f. But when the values of p_s are used in Eq. 104, the corresponding values of C more nearly agree with the orders 0.25, 0.50, and 0.75 of the quartiles which were to be found.

TABLE I

LOWER ONE-SIDED 0.975 CONFIDENCE LIMITS (C) FOR THE PROBABILITY OF THE NON-OCCURRENCE OF AN EVENT PER TRIAL ($1-p_s$) BASED ON OCCURRENCES (n_f) IN INDEPENDENT TRIALS (n_t)

n_t	n_f	POISSON DISTRIBUTION		BINOMIAL DISTRIBUTION	
		APPROXIMATION By EQ. 105*	TABLES BY PEARSON & HARTLEY (Ref. 20)	APPROXIMATION BY EQ. 108 **	TABLES BY HALD (Ref. 21)
5	0	0.478	0.478	0.478	0.478
5	1	0.353	0.328	0.276	0.284
51	1	0.911	0.896	0.891	0.896
51	6	0.817	0.774	0.779	0.761
51	11	0.785	0.680	0.741	0.646
101	1	0.954	0.946	0.944	0.946
102	2	0.945	0.925	0.932	0.931
102	22	0.785	0.722	0.741	0.692
501	1	0.990	0.989	0.989	0.989

* $p_s = 1 - [(1-C)/e^{n_f}]^{1/(n_t - n_f/2)}$

** $p_s = 1 - [(1-C)/e^{n_f}]^{[(3+2C)/4]^{\delta}/(n_t - n_f/2)}$

$\delta = 0$ when $n_f = 0$

$= 1$ when $n_f \neq 0$

TABLE II

ORDER (C) FOR BINOMIAL PERCENTILES OF APPROXIMATIONS (p_s and p_n) TO THE TOLERANCE QUARTILES FOR THE EVENT PROBABILITY PER TRIAL BASED ON THE NUMBER OF OCCURRENCES (n_f) IN 286 INDEPENDENT TRIALS (n_t).

	First Tolerance Quartile				Second Tolerance Quartile				Third Tolerance Quartile				
n_f	p_s	C(%)	p_n	C(%)	p_s	C(%)	p_n	C(%)	p_s	C(%)	p_n	C(%)	n_f
1	0.0039	31.1	0.0011	4.3	0.0059	50.5	0.0035	26.5	0.0094	74.9	0.0059	50.0	1
2	0.0070	32.4	0.0037	8.9	0.0094	50.5	0.0070	32.4	0.0133	73.3	0.0103	56.8	2
3	0.0101	32.5	0.0064	11.4	0.0129	50.4	0.0105	35.3	0.0172	72.6	0.0146	60.0	3
4	0.0131	32.3	0.0093	13.0	0.0164	50.4	0.0140	37.2	0.0211	72.3	0.0187	62.0	4
5	0.0162	31.9	0.0123	14.2	0.0199	50.4	0.0175	38.5	0.0250	72.2	0.0227	63.4	5
6	0.0193	31.4	0.0153	15.0	0.0234	50.4	0.0210	39.5	0.0289	72.3	0.0267	64.4	6
7	0.0223	30.9	0.0183	15.7	0.0269	50.3	0.0245	40.2	0.0329	72.4	0.0307	65.3	7
8	0.0254	30.4	0.0214	16.3	0.0304	50.3	0.0280	40.8	0.0368	72.6	0.0346	65.9	8
9	0.0285	29.9	0.0245	16.8	0.0338	50.3	0.0315	41.4	0.0407	72.9	0.0385	66.4	9
10	0.0315	29.4	0.0276	17.2	0.0373	50.3	0.0350	41.8	0.0446	73.1	0.0423	66.9	10
11	0.0346	28.9	0.0308	17.6	0.0408	50.3	0.0385	42.2	0.0485	73.4	0.0462	67.3	11
12	0.0377	28.4	0.0340	17.9	0.0443	50.3	0.0420	42.5	0.0524	73.7	0.0500	67.7	12
13	0.0407	28.0	0.0372	18.1	0.0478	50.2	0.0455	42.8	0.0563	74.0	0.0538	68.0	13
14	0.0438	27.5	0.0404	18.4	0.0513	50.2	0.0490	43.1	0.0601	74.3	0.0476	68.2	14
15	0.0469	27.0	0.0436	18.6	0.0548	50.2	0.0525	43.3	0.0641	74.6	0.0614	68.5	15
16	0.0500	26.6	0.0468	18.8	0.0583	50.2	0.0560	43.5	0.0679	74.9	0.0652	68.7	16
17	0.0531	26.2	0.0500	19.0	0.0618	50.2	0.0595	43.7	0.0718	75.2	0.0690	68.9	17
18	0.0561	25.7	0.0533	19.2	0.0653	50.2	0.0630	43.9	0.0757	75.5	0.0727	69.1	18
19	0.0592	25.3	0.0565	19.3	0.0687	50.1	0.0665	44.1	0.0796	75.7	0.0765	69.3	19
20	0.0623	24.9	0.0598	19.5	0.0722	50.1	0.0700	44.2	0.0834	76.0	0.0802	69.4	20
21	0.0654	24.5	0.0630	19.6	0.0757	50.1	0.0735	44.4	0.0874	76.3	0.0839	69.6	21
22	0.0685	24.1	0.0663	19.8	0.0792	50.1	0.0770	44.5	0.0912	76.6	0.0877	69.7	22
23	0.0715	23.8	0.0696	19.9	0.0827	50.1	0.0805	44.6	0.0951	76.9	0.0914	69.9	23
24	0.0746	23.4	0.0729	20.0	0.0862	50.1	0.0840	44.8	0.0990	77.1	0.0951	70.0	24
25	0.0777	23.0	0.0762	20.1	0.0897	50.0	0.0875	44.9	0.1029	77.4	0.0988	70.1	25
26	0.0808	22.7	0.0795	20.2	0.0931	50.0	0.0910	45.0	0.1067	77.6	0.1025	70.2	26
27	0.0839	22.3	0.0828	20.3	0.0966	50.0	0.0945	45.1	0.1106	77.9	0.1062	70.3	27
28	0.0870	22.0	0.0861	20.4	0.1001	50.0	0.0980	45.2	0.1144	78.1	0.1099	70.4	28
29	0.0901	21.6	0.0894	20.5	0.1036	50.0	0.1015	45.3	0.1183	78.4	0.1136	70.5	29
30	0.0932	21.3	0.0927	20.6	0.1071	50.0	0.1050	45.4	0.1222	78.6	0.1173	70.6	30
31	0.0963	21.0	0.0960	20.6	0.1106	49.9	0.1085	45.4	0.1260	78.9	0.1209	70.7	31
32	0.0993	20.7	0.0994	20.7	0.1140	49.9	0.1120	45.5	0.1299	79.1	0.1246	70.7	32
33	0.1024	20.4	0.1027	20.8	0.1175	49.9	0.1155	45.6	0.1337	79.3	0.1283	70.8	33
34	0.1055	20.1	0.1060	20.9	0.1210	49.8	0.1190	45.7	0.1376	79.5	0.1319	70.9	34
35	0.1086	19.8	0.1094	20.9	0.1245	49.8	0.1225	45.7	0.1414	79.7	0.1356	71.0	35

$$p_n = \bar{p}_n \pm 0.6745 \sqrt{\bar{p}_n (1-\bar{p}_n)/n_t} \quad \text{where } \bar{p}_n = n_f/n_t$$

$$p_s = 1 - [(\tfrac{1}{2} \pm \tfrac{1}{4})/e^{n_f}] (1 \pm 1/8)(n_t - n_f/2) \quad \text{where } n_f \neq 0$$

} ± is -, nil, and + for 1st, 2nd, and 3rd quartiles respectively

APPENDIX C. CRATER DEPTH

The purpose of this appendix is to establish the necessary extension of the crater depth formula

$$p_0 \sim m^{\frac{1}{3}} (v_c \cos x_2)^{y_4} \tag{109}$$

which was developed in Section II.D.3 (Eq. 47).

Herrmann and Jones' [14] survey and analysis of published theoretical and empirical results for the crater depth in thick metal plates by hypervelocity projectiles are believed to provide a sufficient basis for establishing the crater shape factor. They conclude that, above a velocity transition region which depends on the target and projectile densities, the projectile strength does not affect penetration, particularly for ductile projectiles, and: "If this is true, then the only factor to account for differences in penetration in a given target material by different projectile materials is the projectile density." By an analysis of the empirical results published for many different target and projectile materials, Herrmann and Jones [14] developed the following empirical non-dimensional penetration law for normal impact:

$$p_0/d = (0.36 \pm 0.07) (\rho_p/\rho_t)^{\frac{2}{3}} (\rho_t v_c^2/H_t)^{\frac{1}{3}} \tag{110}$$

where (1) H_t is the Brinell Hardness of the target, (2) ρ_p and ρ_t are the projectile and target densities respectively, and (3) d is the diameter of the projectile. But, when the units for ρ_t are gm/cm^3 and those for v_c are km/sec, then a further proportionality constant is necessary in the last term in Eq. 110 because, by the definition in the Metals Handbook [22], the units for Brinell Hardness H_t are kilograms of force per square millimeter, i.e., Eq. 110 must be replaced by

$$p_0/d = 10^{y_5} (\rho_p/\rho_t)^{\frac{2}{3}} (k\rho_t v_c^2/H_t)^{\frac{1}{3}} \tag{111}$$

where

$$k = \frac{(gm/cm^3)(10^5\ cm/sec)^2}{(980{,}665\ gm\ cm/sec^2)/(10^{-1}\ cm)^2} = 102. \tag{112}$$

Also in Eq. 111, y_7 is an approximately normally distributed random variable, indicating the uncertainty in the relation and in the information about it, determined from the coefficient in Eq. 110 by

$$10^{y_5} = 0.36 \pm 0.07 = \bar{x}_3 \pm \sigma_{x_3} \ , \tag{113}$$

where one assumes from various comments that the numerically indicated uncertainty is standard deviation rather than probable error or mean deviation (mean absolute error). Also, Herrmann and Jones [14] have explained that they got the results, Eqs. 110 and 113, by plotting and fitting on log-log paper. So it is evident that x_3 in Eqs. 110 and 111 is actually the antilogarithm of the more basic random variable y_5. Because it is subject to the normal law of error more directly in the fitting process than is x_3, y_5 can more appropriately be considered as approximately normally distributed. Presumably y_5 can be considered to have mean $\overline{y}_5$ and standard deviation σ_{y_5} given by

$$\overline{y}_5 = \log_{10} 0.36 = -0.44 \tag{114}$$

$$\sigma_{y_5} = \log_{10} (0.36 + 0.07) - \log_{10} 0.36 = 0.08 \quad . \tag{115}$$

Let both p and d in Eq. 111 be measured in centimeters. Then, assuming that meteoroid hazard is not essentially misrepresented by a spherical meteoroid of mass m grams,

$$d = 2(3m/4\pi\rho_p)^{\frac{1}{3}} \quad . \tag{116}$$

The experimental conditions under which the relations given in Eq. 111 were found involved velocities ranging up to 4.88 km/sec (16,000 ft/sec). Then, by Eqs. 111, 113, and 116, crater depth (at normal incidence) would be expressed by

$$p_0 = 2(10^{y_5}\left(\frac{3km}{4\pi H_t}\right)^{\frac{1}{3}} (4.88)^{\frac{2}{3}} (\rho_p/\rho_t)^{\frac{1}{3}}\left(\frac{v_c}{4.88}\right)^{\frac{2}{3}} \tag{117}$$

Herrmann and Jones [14] make the following further comment about Eq. 110: "It might be noted that a slightly higher exponent in ρ_t might be expected to fit slightly better. However, it was decided to retain the advantages of a non-dimensional fit. Small changes (±10 percent) in exponents of the non-dimensional parameters did not significantly alter the mean deviation." Also, the value to be used for the exponent of (ρ_p/ρ_t) is uncertain, to a considerable extent, as is indicated by Bjork [15]. However, the random coefficient 10^{y_5} in Eq. 117 must account for the uncertainty in the exponents of density and velocity over the density-velocity region involved in the experiments. Some further uncertainty because of extrapolation to higher velocities is represented by replacing the velocity ratio exponent in Eq. 117 by y_4 as in Eq. 109. Therefore (by Eqs. 109, 112, and 117) thick-target crater depth at oblique incidence is

$$p_0 = 10^{1.222 - 0.688y_4 + y_5}\left(\frac{\rho_p m}{\rho_t H_t}\right)^{\frac{1}{3}} (v_c \cos x_2)^{y_4} \quad . \tag{118}$$

It is of some interest to see how well crater depth (by Eq. 118) agrees with the following formula established by Bjork [15] for the depth of craters in thick aluminum targets hit by aluminum projectiles at normal incidence:

$$p_0 = 1.09\ (m v_c)^{\frac{1}{3}} . \qquad (119)$$

In establishing Eq. 119 Bjork [15]: (1) obtained the functional dependence by theoretical considerations and (2) chose the coefficient for agreement with experimental results at 6.3 km/sec. He did not report the Brinell hardness of the aluminum target. But, for soft aluminum with Brinell hardness 40, Eqs. 118 and 119 indicate the same median value for the 6.3 km/sec impact velocity when the median values of y_4 and y_5, by Eqs. 44 and 114 respectively are substituted into Eq. 118.

REFERENCES

1. Hawkins, G.S., and R.B. Southworth, "The Statistics of Meteors in the Earth's Atmosphere," Smithsonian Contributions to Astrophysics, Vol. 2, No. 11, 1958, Smithsonian Institution, Washington, D.C.

2. Nysmith, C., and J.L. Summers, "Preliminary Investigation of Impact on Multiple-Sheet Structures and an Evaluation of the Meteoroid Hazard to Space Vehicles," NASA Technical Note D-1039, September 1961.

3. Whipple, F.L., "On Meteors and Penetration," Paper Presented at the National Meeting of the American Astronautical Association in Los Angeles, California, January 15-17, 1963. (Paper Preprint: January 8, 1963 at the Smithsonian Astrophysical Observatory, Cambridge, Mass.).

4. Whipple, F.L., "The Meteoritic Risk to Space Vehicles," Vistas in Astronautics (First Annual Air Force Office of Scientific Research Astronautics Symposium), Ed., Alperin, M., and Sterm, M., Pergamon Press, 1958, pp. 115-124.

5. Laevastu, T., and O. Mellis, "Size and Mass Distribution of Cosmic Dust," Journal of Geophysical Research, Vol. 66, No. 8, August 1961, pp. 2507-2508.

6. Dubin, M., "IGY Micrometeorite Measurements," Space Research, pp. 1042-1058, 1960.

7. Dubin, M., "Meteoritic Dust Measured from Explorer I," Annals of the International Geophysical Year, Vol. XII, Part II, Pergamon Press, 1960, pp. 472-484.

8. Beard, D.B., "Interplanetary Dust Distribution and Erosion Effects," Surface Effects on Spacecraft Materials, 1st Symposium Ed., Clauss, F.J., 1960, pp. 378-390.

9. Siedentopf, H., "Diffuse Matter in the Solar System," Meteors (A Symposium on Meteor Physics): Special Supplement (Vol. 2) to the Journal of Atmospheric and Terrestrial Physics, Ed., Kaiser, T.R., Pergamon Press, 1955, pp. 145-146.

10. Best, G.T., "The Accretion of Meteoritic Material by the Earth," Space Research, Proceedings of the First International Space Science Symposium, Ed., Bijl, H.K., Interscience Pub., 1960 pp. 1023-1032.

11. Watson, F.G., "Between the Planets," Harvard University Press, Cambridge, Mass., 1952.

12. Rinehart, J.S., "Meteor Distribution and Cratering," Proceedings of the Second Hypervelocity and Impact Effects Symposium (see Ref. 25), pp. 45-53.

13. Eichelberger, R.J., and J.W. Gehring, "Effects of Meteoroid Impacts on Space Vehicles," American Rocket Society Paper No. 2030-61, Space Flight Report to the Nation, October 9-15, 1961.

14. Herrmann, W., and A.H. Jones, "Survey of Hypervelocity Impact Information," Aeroelastic and Structures Research Laboratory, Massachusetts Institute of Technology, Report No. 99-1, September 1961.

15. Bjork, R.L., "Meteoroids versus Space Vehicles," ARS Journal, June 1961, Vol. 31, No. 6, pp. 803-807.

16. Hoenig, S.A., and A. Ritter, "Problems in the Meteoric Erosion," Proceedings of the Second Hypervelocity and Impact Effects Symposium, Vol. 1, Ed., Mannix, W.C., et.al., December 1957, pp. 57-68.

17. Black, S.D., "Setting the Structural Design Criteria for Space Debris Effects in Cislunar and Outer Space Travel," Society of Automotive Engineers, National Aeronautic Meeting Report 520E, April 3-6, 1962.

18. McKinley, D.W.R., Meteor Science and Engineering, 1961, McGraw-Hill Book Co., Inc.

19. Lloyd, D.K., and M. Lipow, Reliability: Management, Methods, and Mathematics, Prentice-Hall, Inc., Englewood Cliffs, N.J., 1962.

20. Pearson, E.S., and H.O. Hartley, Biometrika Tables for Statisticians, Volume 1, Cambridge University Press, Cambridge, England, 1954.

21. Hald, A., Statistical Tables and Formulas, John Wiley & Sons, New York, N.Y., 1952.

22. "Metals Handbook," American Society of Metals, 1948.

George C. Marshall Space Flight Center
National Aeronautics and Space Administration
Redstone Arsenal, Huntsville, Alabama
August, 1963